

Copyright
by
Travis Kimble Imken
2014

The Thesis committee for Travis Kimble Imken
Certifies that this is the approved version of the following thesis:

**Design and Characterization of a Printed Spacecraft
Cold Gas Thruster for Attitude Control**

APPROVED BY

SUPERVISING COMMITTEE:

E. Glenn Lightsey, Supervisor

Andrew Klesh

**Design and Characterization of a Printed Spacecraft
Cold Gas Thruster for Attitude Control**

by

Travis Kimble Imken, B.S.As.E

THESIS

Presented to the Faculty of the Graduate School of
The University of Texas at Austin
in Partial Fulfillment
of the Requirements
for the Degree of

MASTER OF SCIENCE IN ENGINEERING

THE UNIVERSITY OF TEXAS AT AUSTIN

May 2014

To my parents and Marissa, thank you for always listening.

Acknowledgments

Dr. E. Glenn Lightsey, who first trusted me to design a satellite when I was a freshman and led me to become the engineer I am today.

Henri, Guru Emeritus, for establishing an incredible working culture in the Lab and allowing me to grow as a leader.

Terry Stevenson, for sharing my burden of stress when assembling Castor and Pollux and reassuring me when neither of us knew what went wrong.

Ben Ayton and Kellen Wall for helping babysit each unit.

Allen Kummer for being my summer mentor and introducing me to JPL.

Parker Francis and Sean Horton for doing the hard tasks and making me laugh when timelines were tight.

Ofer Eldad, Shaina Johl, Andrew Fear, Chris McBryde, Katharine Gamble, and Karl McDonald for your support in the Lab and school.

And Jonathan Lumang, for making sure I always had dinner company.

Design and Characterization of a Printed Spacecraft Cold Gas Thruster for Attitude Control

Travis Kimble Imken, M.S.E.
The University of Texas at Austin, 2014

Supervisor: E. Glenn Lightsey

A three-rotational degree of freedom attitude control system has been developed for the NASA Jet Propulsion Laboratory's INSPIRE Project by the Texas Spacecraft Laboratory at The University of Texas at Austin. Using 3D plastic printing manufacturing techniques, a cold gas thruster system was created in order to detumble and maintain the attitude of two 3U CubeSats traveling through interplanetary space. A total of four thruster units were produced, including two engineering designs and two flight units. The units feature embedded sensors and millisecond level thrust control while using an inert, commercially-available refrigerant as a propellant. The thrust, minimum impulse bit, and specific impulse performance of the cold gas units was characterized using a ballistic pendulum test stand within a microtorr vacuum chamber. A heating element was used to change the temperature conditions of the propellant and determine the relationship between temperature and performance. The flight units were delivered in January of 2014 and the INSPIRE satellites are expected to launch in the upcoming year.

Table of Contents

| | |
|---|-----------|
| Acknowledgments | v |
| Abstract | vi |
| List of Tables | x |
| List of Figures | xi |
| Chapter 1. Introduction | 1 |
| 1.1 The CubeSat Standard | 2 |
| 1.2 Contributions | 2 |
| 1.3 Thesis Organization | 3 |
| Chapter 2. Motivation | 5 |
| 2.1 Texas Spacecraft Laboratory | 6 |
| 2.2 Cold Gas Thruster Systems | 8 |
| 2.3 3D Printing Technology | 9 |
| 2.4 Past 3D Printed CG Systems | 12 |
| 2.4.1 MEPSI | 12 |
| 2.4.2 LONESTAR Mission 2: Bevo-2 | 14 |
| 2.5 The INSPIRE Mission and Requirements | 16 |
| Chapter 3. Trades and Design | 18 |
| 3.1 Component Selection and Trade Studies | 18 |
| 3.1.1 Propellant Options | 18 |
| 3.1.2 New Materials | 21 |
| 3.1.3 Valves | 21 |
| 3.1.4 Sensors | 23 |
| 3.2 INSPIRE Thruster Design | 26 |
| 3.2.1 EDU Design | 26 |

| | | |
|-------------------|--|-----------|
| 3.2.2 | FTT Design | 30 |
| 3.2.3 | The Flight Units | 34 |
| 3.2.4 | Filling and Ground Support Equipment | 34 |
| Chapter 4. | Description of Test Equipment | 39 |
| 4.1 | Approach and Methodology | 39 |
| 4.2 | The Vacuum Chamber Setup | 40 |
| 4.3 | Test Stands | 43 |
| 4.3.1 | EDU Test Stand | 43 |
| 4.3.2 | Flight Collection Stand | 44 |
| 4.4 | LabView Controllers | 46 |
| 4.5 | Calibration Methodology | 47 |
| Chapter 5. | Thrust Determination and Analysis | 50 |
| 5.1 | Collection Methods | 50 |
| 5.1.1 | Setup | 51 |
| 5.1.2 | Conditions | 52 |
| 5.1.3 | Supporting Hardware Challenges | 56 |
| 5.1.4 | Presentation of Data | 59 |
| 5.1.5 | Best Fit Lines | 60 |
| 5.2 | Thrust Determination Data | 61 |
| 5.2.1 | Room Temperature | 61 |
| 5.2.2 | Heated Tests | 64 |
| 5.2.2.1 | Below Saturation Pressure | 65 |
| 5.2.2.2 | At Saturation Pressure | 69 |
| 5.2.3 | Summary of Results | 72 |
| 5.3 | Combined Results | 72 |
| 5.3.1 | Thrust Determination | 73 |
| 5.3.2 | Specific Impulse | 76 |
| 5.3.3 | Minimum Impulse Bit | 77 |
| 5.4 | Analysis of Results | 77 |

| | |
|--|-----------|
| Chapter 6. Lessons Learned and Recommendations | 81 |
| 6.1 Lessons Learned | 81 |
| 6.2 Designs beyond INSPIRE | 83 |
| 6.2.1 Adapting the Design for Other Missions | 83 |
| 6.2.2 Scaling the Technology | 85 |
| 6.3 Further Investigations | 87 |
| 6.3.1 New Materials and Manufacturing | 87 |
| 6.3.2 Improved Test Stand | 89 |
| 6.3.3 Miniature Components | 90 |
| 6.3.4 Long Term Duration Tests | 92 |
| 6.4 The Thruster Model | 93 |
| Chapter 7. Conclusion | 95 |
| Bibliography | 96 |
| Vita | 99 |

List of Tables

- 5.1 Thermal Test Steady State Temperatures 52
- 5.2 Pressure Transducer Calibration 53
- 5.3 Summary of testing results for each run 73
- 5.4 Room Temperature Performance of the Thruster 79

List of Figures

| | | |
|------|--|----|
| 1.1 | JPL/TSL's RACE Satellite (left) [3] and a NanoRacks Deployment(right) [4] | 3 |
| 2.1 | The Bevo-2 satellite, disassembled on the clean bench | 7 |
| 2.2 | 3D printed brake cooling duct for the Renault F1 team [10] | 10 |
| 2.3 | INSPIRE EDU Thruster Assembly Cross Section featuring internal piping and fully enclosed tanks | 11 |
| 2.4 | MEPSI-3 Flight 3D Printed CG Thruster | 13 |
| 2.5 | The Bevo-2 thruster being assembled before a leak check [3] | 15 |
| 3.1 | Cut open plastic manifold after a propellant compatibility test | 20 |
| 3.2 | Accura Bluestone printing of the EDU plastic manifold | 22 |
| 3.3 | The extended performance solenoid valve from The Lee Company [23] | 23 |
| 3.4 | Omega PX600 miniature pressure transducer [24] | 25 |
| 3.5 | Different valve combinations for different maneuvers | 27 |
| 3.6 | The EDU CAD design (left) and the assembled EDU | 28 |
| 3.7 | Impedance matched piping shown on an EDU cross-section | 29 |
| 3.8 | Angled and canted 3D printed FTT thruster nozzles | 31 |
| 3.9 | The FTT fill and drain valves | 32 |
| 3.10 | FTT fittings, filters, and controlling electronics | 33 |
| 3.11 | The flight INSPIRE ACS units (RACE and Bevo-2 in background) | 35 |
| 3.12 | Fill and drain valve for the INSPIRE flight units [25] | 36 |
| 3.13 | Interface between the filling equipment and the thruster | 37 |
| 4.1 | The TSL's microtorr vacuum chamber | 41 |
| 4.2 | The heating plate for the vacuum chamber | 42 |
| 4.3 | The test chamber and stand for the EDU | 44 |
| 4.4 | The FTT with the test stand in the vacuum chamber | 45 |
| 4.5 | The LabView VI to measure pendulum deflection | 47 |

| | | |
|------|--|----|
| 5.1 | Pressure ADC calibration | 55 |
| 5.2 | Refrigerant Properties in Tested Range [18] | 56 |
| 5.3 | Thrust differences based on sample time | 58 |
| 5.4 | Room temperature test at saturation pressure | 62 |
| 5.5 | Room temperature with the PADC at 300 | 63 |
| 5.6 | Room temperature with PADC at 200 | 64 |
| 5.7 | Heated run 1 with PADC at 415 | 65 |
| 5.8 | Heated run 2 with PADC at 415 | 66 |
| 5.9 | Heated run 3 with PADC at 415 | 67 |
| 5.10 | Heated run 4 with PADC at 415 | 68 |
| 5.11 | Heated run 1 at saturation pressure | 69 |
| 5.12 | Heated run 2 at saturation pressure | 70 |
| 5.13 | Heated run 3 at saturation pressure | 71 |
| 5.14 | Heated run 4 at saturation pressure | 72 |
| 5.15 | All data for PADC 415 | 74 |
| 5.16 | Thrust compared to expansion tank pressure | 75 |
| 6.1 | A baselined 1U 6-DOF thruster | 86 |
| 6.2 | The FTT fill valve and volume cutout | 91 |

Chapter 1

Introduction

Initially developed to allow students to fly their own hardware in space, CubeSats have become capable spacecraft platforms for scientific payloads, technology demonstrations, and military missions. Programs within NASA, the military, the National Science Foundation, and dozens of universities are investing resources into producing a spacecraft that can perform valuable missions in a miniature form factor. While larger spacecraft are constrained by the farring diameter on a large rocket, the compact size of a CubeSat places an inherent limitation on the power generation capability, volume available for payloads, and fidelity of attitude control systems. Like larger spacecraft, there are many options available for attitude control, including reaction wheels, solar sails, magnetorquers, or thrusters. However, with volume constrained CubeSats, there is a need for an attitude control system that can be customized around other hardware components and be quickly reconfigurable as the design matures. The development of a 3D printed cold gas attitude control system for the JPL INSPIRE CubeSat mission has demonstrated this modularity while delivering a functional attitude control system. This chapter provides an overview of the CubeSat standard, the contributions of the research, and the organization of the thesis.

1.1 The CubeSat Standard

The CubeSat standard was created as a collaboration between California Polytechnic University and Stanford University to reduce cost and development time of picosatellites while enabling increased student access to space. The CubeSat standard is measured in units, where a 1-Unit (or 1U) section is roughly a 10cm cube with a mass around $1\frac{1}{3}\text{kg}$ [1]. CubeSats are traditionally delivered into space as secondary payloads in fully enclosed, containerized launchers known as deployers. As part of the CubeSat standard, Cal Poly developed the Poly Picosatellite Orbital Deployer (P-POD). The P-POD can carry up to a 3U volume of satellites, which could be three separate satellite payloads or a single larger satellite. The satellites are ejected from the deployer units after the primary payload has been placed into orbit by the launch provider; as a result, CubeSat developers have low-cost access to space but will be in an orbit close to that of the primary payload. CubeSats have other deployment options, including deployment off the ISS through NanoRacks after being delivered to the station as cargo through a resupply vessel [2]. A picture of the RACE 3U CubeSat and a NanoRacks deployment module used on the ISS is shown in Figure 1.1.

1.2 Contributions

The purpose of this thesis is to introduce the reader to the design, development, and validation of a 3D-printed Cold Gas (CG) thruster for attitude control of a CubeSat. This unit was developed at the University of

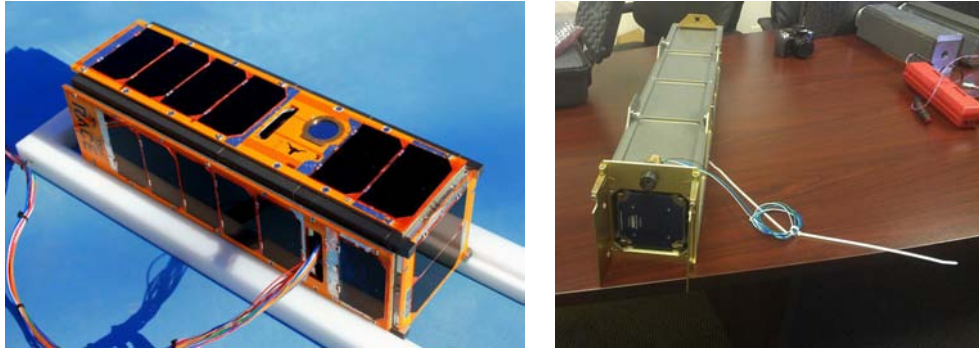


Figure 1.1: JPL/TSL’s RACE Satellite (left) [3] and a NanoRacks Deployment(right) [4]

Texas at Austin’s Texas Spacecraft Laboratory (TSL) as part of a year-long collaboration with the Jet Propulsion Laboratory (JPL) for the Interplanetary NanoSpacecraft Pathfinder In Relevant Environment (INSPIRE) Project. This project consists of two, identical 3U CubeSats that will be deployed in an Earth escape orbit. The satellites will “open deep-space heliophysics and planetary science to the CubeSat community by demonstrating functionality, communication, navigation and payload-hosting in interplanetary space” [5]. The TSL was responsible for designing and producing two CG Attitude Control Systems (ACS) to detumble the satellites after deployment and maintain spacecraft attitude during operations. These units were delivered to JPL in January of 2014.

1.3 Thesis Organization

This thesis is organized into seven chapters. Chapter 2 discusses the small spacecraft heritage of the Texas Spacecraft Laboratory and introduces

the cold-gas thruster technology, 3D printing concepts and advantages, highlights a quick survey of 3D printed CG thrusters, and summarizes the INSPIRE mission and attitude control system requirements. Chapter 3 describes the trade studies and component decisions that drove the design of the thruster units and also highlights the design features and improvements from the first engineering design to the flight units. Chapter 4 introduces the concept of the ballistic pendulum test stand used to characterize the thrusters performance and highlights how data was collected as well as a summary of the TSL's vacuum chamber. Chapter 5 presents the methodology behind the thrust data collection, relays challenges related to the thruster support equipment, and includes all of the collected data with analysis. Chapter 6 begins with lessons learned and goes into a reflection on the development of the thruster units, highlighting the flexibility of these units in other satellites and illustrating how the units may continue to evolve. Chapter 7 concludes the thesis with thoughts about the engineering process and goals for the future.

Chapter 2

Motivation

Small spacecraft are playing a game changing role in the development and demonstration of spacecraft technologies as well as fulfilling valuable science, military, and commercial mission roles. This evolution has been fueled by innovations in the miniaturization of electronics, an increased number of companies marketing products targeted at the small satellite community, and novel manufacturing techniques are making CubeSats a useful platform. CubeSat missions to low Earth orbit are common but no mission has yet to leave Earth's orbit. As CubeSat missions are baselined to explore the Moon, near-Earth objects, and other planets, cold gas attitude control systems have the potential to play an increasingly important role. Outside of Earth's magnetic field, a CG thruster system can replace magnetorquers to desaturate reaction wheels. These systems could replace energy consuming and expensive reaction wheels to keep spacecraft antennas directed at Earth.

3D printed CG thruster technology has been proven to work in space [6] and will benefit the attitude capabilities of small spacecraft. Up to this point, the limiting factor in the technology is a lack of knowledge about the fineness of control, reliability of the systems over the mission lifetime, and scalability of the technology. This thesis focuses on the research around the development

and characterization of the INSPIRE attitude control systems.

2.1 Texas Spacecraft Laboratory

The Texas Spacecraft Laboratory, formerly known as the Satellite Design Laboratory, is a funded research laboratory within the Aerospace Engineering and Engineering Mechanics Department at The University of Texas at Austin. The TSL's Principle Investigator is Dr. Glenn Lightsey and is comprised of about ten graduate and twenty undergraduate students. The TSL has launched three satellites; The Bevo-1 satellite was part of the NASA Johnson Space Center LONESTAR (Low Earth Orbiting Navigation Experiment for Spacecraft Testing Autonomous Rendezvous and docking) Program with Texas A&M. Bevo-1 was launched aboard Space Shuttle Endeavor in May 2009 and was a 5-inch cube. The TSL also launched the two FASTRAC (Formation Autonomy Spacecraft with Thrust, Relnav, Attitude, and Crosslink) satellites. These spacecraft were larger, nanosatellite sized vehicles (under 100kg total) and were launched on STP-S26 in Fall 2010 to perform cross-link relative navigation.

As of Spring 2014, the TSL continues to work on several more CubeSat missions. The 3U-sized Bevo-2 satellite is the follow-up mission to the Bevo-1 spacecraft. Bevo-2 is expected to launch in 2014 and will demonstrate a six degree-of-freedom Guidance, Navigation, and Control (GN&C) system that includes an attitude determination and control system as well as a small cold gas thruster [7]. Figure 2.1 shows the partially assembled Bevo-2 spacecraft with the blue cold gas thruster module visible in the middle unit. The TSL

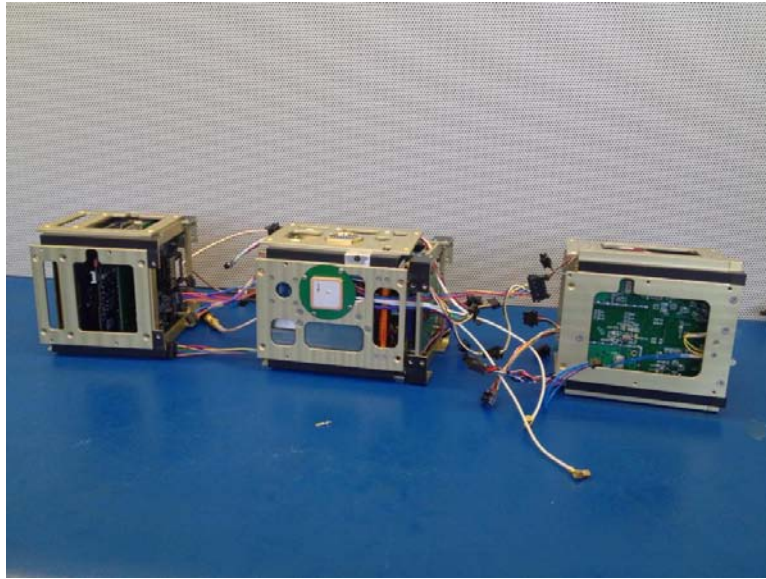


Figure 2.1: The Bevo-2 satellite, disassembled on the clean bench

has also assembled and delivered the RACE (Radiometer Atmospheric CubeSat Experiment) 3U CubeSat in 2014 to JPL. RACE features a TSL-designed structure, bus, and interface suite to integrate with a JPL provided radiometer scientific payload. This $183GHz$ radiometer will look at atmospheric water vapor and advance the technology of the $35nm$ indium phosphide receiver of the radiometer [8] and is also expected to launch in 2014. Finally, the TSL is also finalizing the design for the ARMADILLO (Atmosphere Related Measurements And Detection of submILLimeter Objects) 3U CubeSat. ARMADILLO won the Air Force Research Laboratory's University Nanosat Program 7 competition in December of 2012. ARMADILLO features a Baylor University provided piezo dust detector to measure small impacts of space debris and will also perform GPS radio occultation with a UT Austin designed dual frequency GPS receiver. ARMADILLO is expected to launch in 2015.

Beyond building integrated satellite missions, the TSL is involved in the development of specialized satellite subsystems. In the past few years, the TSL has gained experience in the design, assembly, and verification of cold gas thruster systems using a 3D manufacturing processes. These systems have been created for translational and attitude maneuvers and use a refrigerant as a propellant. The TSL is able to test these systems using the TSL's in-lab microtorr vacuum chamber.

2.2 Cold Gas Thruster Systems

Cold gas thruster systems are used as actuators on spacecraft and can provide translational maneuvers, rotational attitude control, or both depending on the configuration. The term 'cold-gas' comes from the use of an inert, non-explosive propellant. The systems are relatively simple in design and thrust is generated by the controlled release of a gaseous propellant. The propellant can be stored as a high pressure gas, such as gaseous nitrogen, or as a saturated liquid, such as a refrigerant. A series of valves control the propellant until the gas is ultimately fired through a nozzle to create a force. These systems feature a low impulse bit, contamination-free propellants, comparatively safe operating conditions, and have been flown in space since the 1960's [9].

CG propulsion systems are one of a few options for CubeSat change in velocity (ΔV) and attitude control maneuvers because the simplicity, safety, and size of the systems closely aligns with the CubeSat design philosophy. The systems can be configured to be low power, designed to address pressure vessel requirements from launch providers, and provide notable performance with a

small percentage of a CubeSat’s volume; for example, a CG thruster system could be used to extend the lifetime of a CubeSat mission in low Earth orbit that might otherwise deorbit due to atmospheric drag.

2.3 3D Printing Technology

3D printing is an additive manufacturing process where a material is built up layer by layer to create a solid, single part. 3D printing encompasses a variety of materials, including different plastics, metals, and other “digital materials” that combine materials to get different durometer properties [11]. This is compared to a more traditional removal machining process, where a part is created from a piece of stock by removing material through a series of cuts. 3D printing allows for parts to be designed and printed in a way that could never be reproduced by a traditional machining processes. This allows the designer to construct geometries such as fully enclosed volumes, complex passageways, and detailed nozzle cones surrounded by a solid piece of printed material. An example of a complex 3D printed part developed for a racing automobile is shown in Figure 2.2.

These 3D printing advantages solve address of the potential issues with past CG systems. Traditional CG thrusters require individual tanks, volume for piping, numerous pressure fittings, and access areas for assembly and spacecraft installation. Each fluidic interface increases the chance for leaks and the physical size of the required hardware introduces volumetric challenges to fit the system within a CubeSat. With 3D printing, a solid piece called a manifold is designed in a way to encompass the storage tanks, piping, and nozzles.



Figure 2.2: 3D printed brake cooling duct for the Renault F1 team [10]

These units are built on a commercially available 3D printer after being designed in a traditional parametric modeling program such as SolidWorks. Once the valves and electronics are mounted onto the manifold and the unit is fueled, the printed CG thruster system has been completely integrated. Figure 2.3 shows a cross section of the Engineering Design Unit (EDU) of the INSPIRE thruster to highlight the enclosed tank volumes and piping passageways that are achievable with the 3D printing technology.

3D printing technologies also further the original goal of the CubeSat standard. A flight-ready 3D printed manifold for a CubeSat thruster can be produced for under \$1,000 and is manufactured in less than a week. In the last decade, the proliferation of 3D printing technologies for the automotive, electrical, and rapid-prototype iteration has led to the introduction of high-

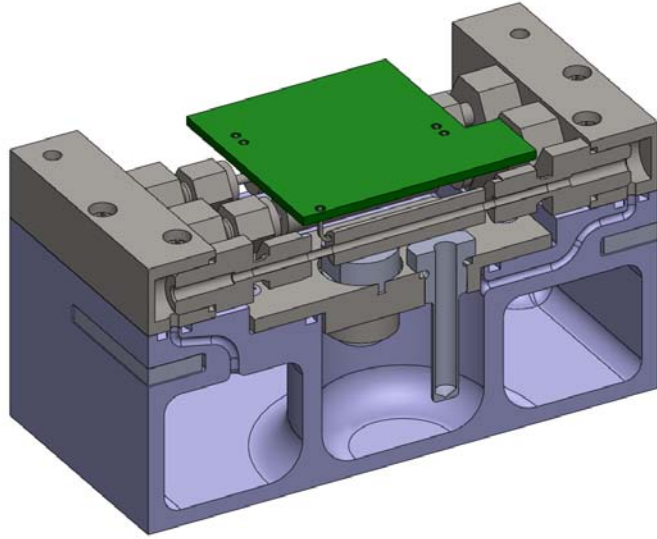


Figure 2.3: INSPIRE EDU Thruster Assembly Cross Section featuring internal piping and fully enclosed tanks

strength materials [12]. The printing technologies are capable of resolutions of only a few milli-inches, comparable to the tolerances used in traditional machine shops. Additionally, the rapid iteration of these units allows CG thruster systems to be infinitely reconfigurable within the host spacecraft or adapted for integration in completely different CubeSats. For example, since the nozzles are printed into the plastic, the manifold can be remanufactured so that a translational nozzle lines up with the spacecraft's center of mass after it has been empirically determined. A 3D printed unit can also fit around other spacecraft components, wiring, and hardware to take advantage of volumes that would otherwise be considered inaccessible or wasted.

2.4 Past 3D Printed CG Systems

The first spacecraft to feature a 3D printed cold gas thruster system was the MEPSI-3 (Microelectromechanical System-based (MEMS) PICOSAT Inspector) mission flown by The Aerospace Corporation on STS-116 in December 2006 [6]. Based on this pioneering implementation of the 3D printing technology, the TSL created a thruster for the Bevo-2 spacecraft in 2009. The Bevo-2 thruster is a 1-DOF system for translational motion and is a technology demonstration of the planned rendezvous and docking maneuvers in the third mission of the LONESTAR program [13].

2.4.1 MEPSI

MEPSI-3 was a 1U cubesat that featured a 3D printed CG propulsion system developed internally by The Aerospace Corporation [6]. The propulsion system was allocated a total mass of 0.5kg and was constructed out of the Somos 11120 stereolithography (SLA) material. The thruster featured three sealed and printed tanks; a main tank stored the bulk of the propellant and was connected via a valve to the first plenum. When that valve was opened, the first plenum was filled with the saturated propellant. With the first valve closed, a second valve opened up between the first and second plenum. The second plenum, called the expansion tank, was much larger in volume so the fluid in the first plenum would expand to a purely gaseous state. This valve was closed, then one of five additional valves opened to direct the propellant out of five nozzles printed into the plastic. Figure 2.4 shows the flight unit of the MEPSI unit.

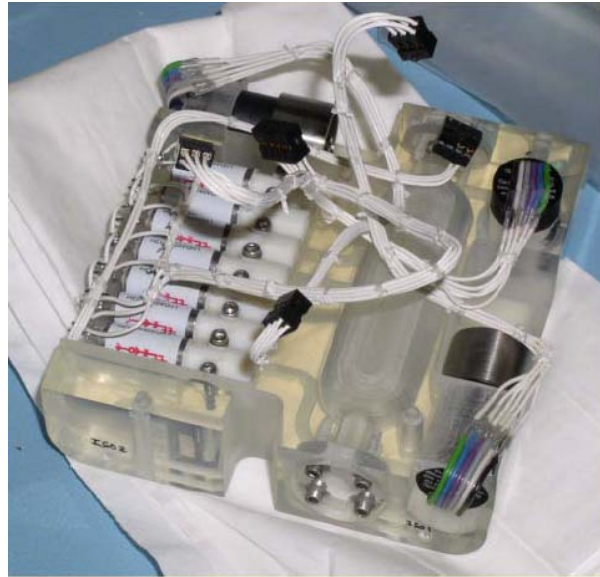


Figure 2.4: MEPSI-3 Flight 3D Printed CG Thruster

The MEPSI-3 satellite was initially planning to carry a common industrial refrigerant from DuPont, Suva R-236fa (R236). This propellant would provide the satellite with an estimated $20 \frac{m}{s}$ of ΔV . However, the orbital analysis showed the satellite could potentially return to the Space Shuttle Orbiter after deployment, so 100 psig Xenon gas was used instead. This lowered the total estimated ΔV to $0.4 \frac{m}{s}$. During its mission, the MEPSI-3 satellite successfully executed and recorded a pulse that changed the satellite's rotation rate. The TSL (at the time called the Satellite Design Laboratory) licensed the technology from The Aerospace Corporation and began development of the next generation of printed CubeSat thrusters.

2.4.2 LONESTAR Mission 2: Bevo-2

The Bevo-2 mission features a full 6-degree of freedom CubeSat GN&C module, including three reaction wheels, gyroscopes, magnetorquers, two digital sun sensors, a magnetometer, a GPS receiver, and a star tracker camera. In addition to these sensors and actuators, the Bevo-2 CubeSat is carrying a 1-DOF thruster that occupies about 0.4U of volume. The thruster was included on the Bevo-2 mission as a technology demonstration; the LONESTAR-3 mission requires that the UT Austin and Texas A&M satellites to rendezvous and dock several times. The printed CG technology was chosen because of the simplicity of the design, safety features, the flight heritage of the technology, and the ability of a 3D printed manifold to fit around all of the other components within the GN&C module.

The Bevo-2 thruster is similar in principle to the MEPSI thruster and can be seen in Figure 2.5. The unit has three tanks separated by valves, an entirely 3D printed manifold, and a converging-diverging nozzle printed into the plastic. Since the concept of operations for Bevo-2 only required translational motion in one direction, only three valves are used on the unit with the single nozzle placed on axis with the center of mass. The unit is designed to handle the R236 propellant. Building off the results from The Aerospace Corporation, the Bevo-2 thruster has undergone six design iterations and tested a variety of valves and materials [14]. As configured now, the Bevo-2 design features high performance solenoid valves from The Lee Company paired with a high strength nanocomposite SLA plastic called Accura Bluestone.

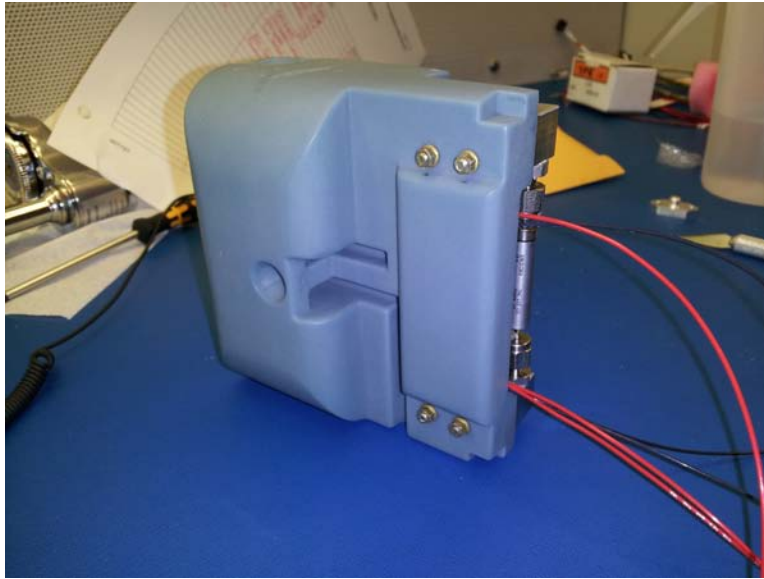


Figure 2.5: The Bevo-2 thruster being assembled before a leak check [3]

Testing of the Bevo-2 thruster is conducted in the TSL's vacuum chamber. A ballistic pendulum test stand is used to measure the total impulse the thruster generated. This was done both by using momentum/energy methods as well as numerically integrating the motion of a pendulum based on the ultimate displacement of the test stand pendulum. When the impulse was divided by the valve pulse duration, the thrust was calculated. It is predicted that Bevo-2 can provide a total of $15\frac{m}{s}$ of ΔV . A finite element analysis was conducted on one iteration of the tank design for the Bevo-2 thruster. The model predicted a burst pressure of 329 psi and was validated with a water burst test conducted in the department. This model ruptured at the computer-predicted location at 328 psia, extremely close to the computer burst prediction. This test showed that computer simulation can be used with good accuracy to predict the factors of safety and pressure characteristics of the

3D printed manifolds [14]. The Bevo-2 thruster also features a first generation of thruster control electronics that include the driving power electronics and a software safety to prevent inadvertent firing. The results of the Bevo-2 thruster testing were published in a paper submitted to the Journal of Small Satellites.

2.5 The INSPIRE Mission and Requirements

The INSPIRE CubeSat mission is a joint mission between JPL, UCLA, The University of Michigan, Cal Poly SLO, The University of Texas at Austin, and the Goldstone-Apple Valley Radio Telescope [15]. The TSL was responsible for the attitude control system and was selected because of the TSL's heritage with 3D printed CG systems and was tasked with modifying the Bevo-2 design into a 3 rotational DOF design. JPL was interested in the technology because the 3D printed system provides "design flexibility and growth of system components until late in the design process" [16]. Because the INSPIRE satellites are sailing beyond Earth orbit, the projected mission lifetime is only a few months, depending on the escape velocity of the launch vehicle. Therefore, it is critical for the attitude control system to maintain a spacecraft orientation such that the X-band antenna will always be pointed back at Earth. Over a year, the TSL created two engineering design units (EDU) and two flight units, which were delivered in January 2014.

The initial requirements for the design of the INSPIRE thruster facilitated an improved design from the Bevo-2 thruster. Firstly, the thruster could only have nozzles shoot out two of the four faces because of solar panel restric-

tions. The thruster also had to match the “footprint” of the CubeSat standard PC-104 board. This included mounting support for four threaded rods that spanned the full 3U length of the spacecraft. A requirement added after the EDU design specified that the thruster had to be filled in a closed loop system to prevent propellant from coming in contact with satellite components; previous versions of the cold gas systems were filled “openly” by chilling the propellant so that its saturation pressure was below room pressure and then pouring the propellant into the unit before sealing the tank. The attitude control algorithm designers also asked the TSL to develop the thruster in a way that would give them both “coarse” control to detumble the satellite after deployment as well as “fine” control to maintain the spacecraft attitude. The thruster also had to incorporate electronics to drive the valves via commands from the main command and data handling computer.

The following chapter discusses the detailed trades and designs for the INSPIRE thruster based on the requirements above.

Chapter 3

Trades and Design

The INSPIRE thruster advanced the state of the art on printed CG thruster design. The initial INSPIRE EDU design was based off of the heritage from the Bevo-2 thruster. This chapter discusses the initial trade studies and decisions for various thruster components as well as walking through the design choices and iterations from conception to flight delivery.

3.1 Component Selection and Trade Studies

Several trade studies were conducted on the thruster propellant, new materials that had been introduced to the market since the Bevo-2 thruster was designed, and valves that would meet the INSPIRE volumetric and performance requirements, as well as a new investigation into sensors that could be embedded into the ACS manifold.

3.1.1 Propellant Options

R236 was initially selected for the INSPIRE mission because of the Bevo-2 heritage. The refrigerant is readily available, easily storable in cylinders, and is non-toxic. It is also cross-marketed as fire extinguisher FE-36, which is suitable for use in areas with people, including hospitals, libraries,

and banks, and laboratories [17]. This helps address safety concerns as a propellant for both personnel and the spacecraft. R236 is a comparatively low pressure refrigerant and is stored as a saturated liquid. This means that the refrigerant will have liquid and gaseous states and that the maximum exerted pressure is only a function of temperature. At room temperature, R236 is only about 35 psia. At a theoretical maximum spacecraft temperature of 55°C , the pressure of R236 is 97 psia [18]. As a comparison, NASA Standard 5003 states that a pressure vessel is a container that will experience a mean design pressure greater than 100 psia [19]. Therefore, by expanding the saturated liquid into a purely gaseous form, milligrams of the propellant can be expelled to generate a force allowing for maximum thruster performance over the course of the mission.

Other DuPont Suva refrigerants are also available and offer a different performance profile because they have different pressures at a given temperature. Refrigerant 123 offers a room temperature pressure 11.4 psia and a pressure of 37 psia at 55°C [20]. This refrigerant offered the benefits of being easier to handle at room temperature because the saturation pressure is below atmospheric pressure and could be kept as a liquid during loading. However, the reduced pressure meant that less thrust would be generated at a given temperature based off the isentropic flow equations. Refrigerant 124 was also considered and had a room temperature pressure of 49 psia and a pressure of 131.3 psia [21], similar to R236. Finally, Refrigerant 134a, commonly used in car air conditioners and widely available, had a room temperature pressure of 85.9 psia and a maximum pressure of 222.4 psia at 55°C [22]. These three

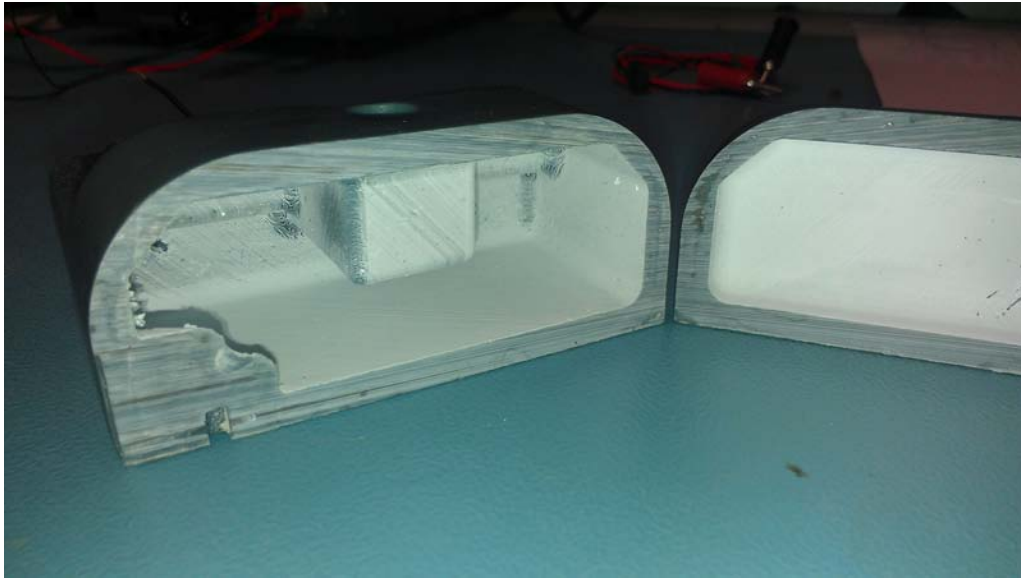


Figure 3.1: Cut open plastic manifold after a propellant compatibility test
alternate refrigerants were similarly inert to R236.

Ultimately the decision was made to stay with R236 because of the pressure profile and design heritage. Material compatibility tests had already been conducted between the SLA plastic and the refrigerant. Figure 3.1 shows a cut open section of a Bevo-2 EDU after the R236 propellant was sealed in the main tank for over 9 months. The plastic showed no deterioration. Also, the higher pressure of R124 and R134a were a potential concern for the primary launch provider. R123 did not have enough pressure potential to fulfill the predicted thrust requirements of the system. Back of the envelope calculations indicated that a projected load of 200g of R236 propellant on the INSPIRE satellites would be several times more than what would be required for the mission.

3.1.2 New Materials

Similarly to the propellant selection, the Accura Bluestone material was initially baselined for INSPIRE because of the design heritage with the Bevo-2 system. The Bluestone material is marketed as a nanocomposite plastic and features exceptional stiffness, very high temperature resistance (over $250^{\circ}C$), and a printing accuracy of 0.004 inches. The material is less dense than aluminum, at $1.78\frac{g}{cm^3}$ compared to $2.7\frac{g}{cm^3}$. The Bluestone has a tensile strength of $66 - 68MPa$, a tensile modulus of $7,600 - 11,700MPa$, and only stretched $1.4\% - 2.4\%$ at break [12]. The vendor that provides the the Bluestone units works with the TSL to print the complex, enclosed geometries free of support material and internal resin. Because the material is opaque, the vendor also ensures that each layer of plastic is free of errors or voids to prevent internal leaking that would not be visible from the outside. The INSPIRE EDU Bluestone unit is shown in Figure 3.2.

Though there are dozens of other SLA materials that could be compared to the Bluestone, the heritage of the Bluestone, the reliability of the manufacturer, and the performance of the material under pressure did not necessitate alternate materials to be investigated. For example, if the Bluestone finite element analysis shows a weakness in specific area of a unit, the model wall could be thickened to handle the increased stress.

3.1.3 Valves

The INSPIRE thruster baselined the extended performance solenoid valves from The Lee Company used on the Bevo-2 satellite. These valves are

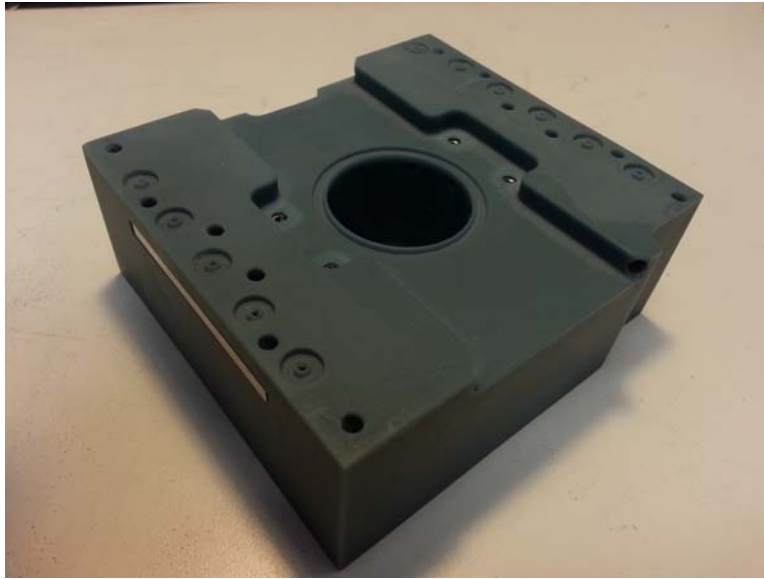


Figure 3.2: Accura Bluestone printing of the EDU plastic manifold

an industry-unique product and are suited for use on the CG thruster systems. The overall size is small, with the solenoid section measuring only 1.3 inches in length and a quarter inch in diameter. The valves are able to actuate repeatedly at $500Hz$, though laboratory experiments at the TSL showed the valve could potentially actuate single pulses faster than $1ms$. Each valve can be driven on a power bus ranging from 5V to 12V is powered off the unregulated battery bus (ranging from 6.4V to 8.4V) on INSPIRE. The maximum rated pressure for the valves is $800psi$ and the seal elastomer is compatible with R236 [23]. Each valve consumes no power when closed and only draws 0.22W under a 10% duty cycle at 5V. Figure 3.3 shows the Lee Company valve.

Similarly to the propellant selection, other valves were briefly considered to replace the Lee Co valves. Over a dozen valves from various brands were investigated for the Bevo-2 satellite and the Lee Co valve performed the



Figure 3.3: The extended performance solenoid valve from The Lee Company [23]

best under the test conditions with the refrigerant. In the end, the extended performance solenoid valves met the requirements of the mission. The initial Bevo-2 assemblies did show a slight leaking issues with the metal to metal fittings improperly secured to the valves, but this was not an issue with the valves themselves.

3.1.4 Sensors

The INSPIRE thruster required a minimum of four nozzles and thus four valves to achieve the 3 rotational DOF. However, because of the interface restrictions with the satellite's threaded rods that passed through the thruster, only a total of five valves could be fit within the allocated volume. The decision was made to forgo the first plenum charging tank and just have a main tank

and expansion tank. This is possible because a single valve can control the flow precisely between the two tanks. To ensure that the gas in the expansion tank is a vapor, temperature and pressure data is needed to compare to the saturation tables for R236. If the pressure is below the saturation pressure, then it is guaranteed that the propellant is in a gaseous state. Currently, electronics cannot be embedded within the plastic during the SLA printing process. As a result, all sensors have to be interfaced into the tank via openings sealed off with o-rings. The expansion tank interface plate for INSPIRE holds a pressure transducer, an NTC thermistor, and a cartridge heater.

The PX600 pressure transducer from Omega was chosen because of the miniature size and performance characteristics. Omega's transducers can be selected to measure 200 to 10,000 psig and output an analog signal. The pressure sensor is hermetically sealed from the propellant environment and is interfaced to an analog to digital converter (ADC) so the data can be read from a satellite data bus. The sensor is shown in Figure 3.4. The TSL modified the sensors for a vacuum environment, including removing outgassing components and characterizing the performance in a hard vacuum. The thermistor was a custom sensor designed by the TSL. A 10K thermistor was potted with a thermally conductive epoxy in an embedded brass probe. This thermistor is connected to a Wheatstone bridge and then to the same ADC as the pressure transducer. The circuit was tuned to measure expansion temperatures from 0 to 50C. The thermistor is very responsive to temperature changes and can detect the "chilling" of the propellant as gas is expelled through the nozzles.

Paired with these sensors, a heater is embedded in a second probe



Figure 3.4: Omega PX600 miniature pressure transducer [24]

housing. The heater is essentially a low-ohm resistor that gets hot when a potential is applied. Ideally, the heater will be used in circumstances where more thrust is desired. By adding energy to the vapor in the expansion tank, the pressure will rise, and more thrust will be generated when the gas is released through a nozzle. The heater can also be used in a situation where the pressure and temperature sensors indicate that some liquid may be in the expansion plenum; for example, this could happen if the satellite cools and causes the propellant to recondense. Raising the temperature with the heater guarantees that only vapor will be expelled. Finally, a current sense resistor is included across the driving power circuitry for the valves. This sensor measures the potential drop across a small resistor and then feeds the signal into the ADC. This allows the main computer to determine how many valves are powered on at a certain time and for how long. This can also be used as a safety check to guarantee that none of the valves are powered when they should not be.

3.2 INSPIRE Thruster Design

The INSPIRE thruster design went through three iterations. The engineering design unit was designed and built in the Spring semester of 2013. The unit was then transferred out to JPL for summer testing in a thermal vacuum chamber. Implementing the lessons learned from the EDU, a second, pre-flight iteration was proposed by the TSL called the Flight Technology Test (FTT) and was built in the Fall of 2013. The FTT implemented new components and helped mitigate any design risks before the flight units were produced. Finally, after testing the FTT and tweaking the final design, the flight units were assembled and tested for the delivery. The FTT remained in Austin for continued thruster characterization testing and the plastic manifold was modified to make it flight-like. The data presented in this thesis was collected from the FTT unit, which is configured identically to the flight units.

3.2.1 EDU Design

The INSPIRE EDU thruster was originally constrained to a total volume of 0.5U. The design includes a plastic manifold with a completely enclosed main tank surrounding an expansion tank that has one open face for the the embedded sensors. Five Lee Company extended performance solenoid valves are secured in a pair of stainless steel manifolds that are bolted onto the plastic manifold with o-rings in a compression fit. These valves control the flow from the main tank to the expansion tank and the flow through each of the four nozzles. Four nozzles are placed on two opposite faces, at 45° angles from the normal. Because the thruster is placed off the center of mass of the satellite,

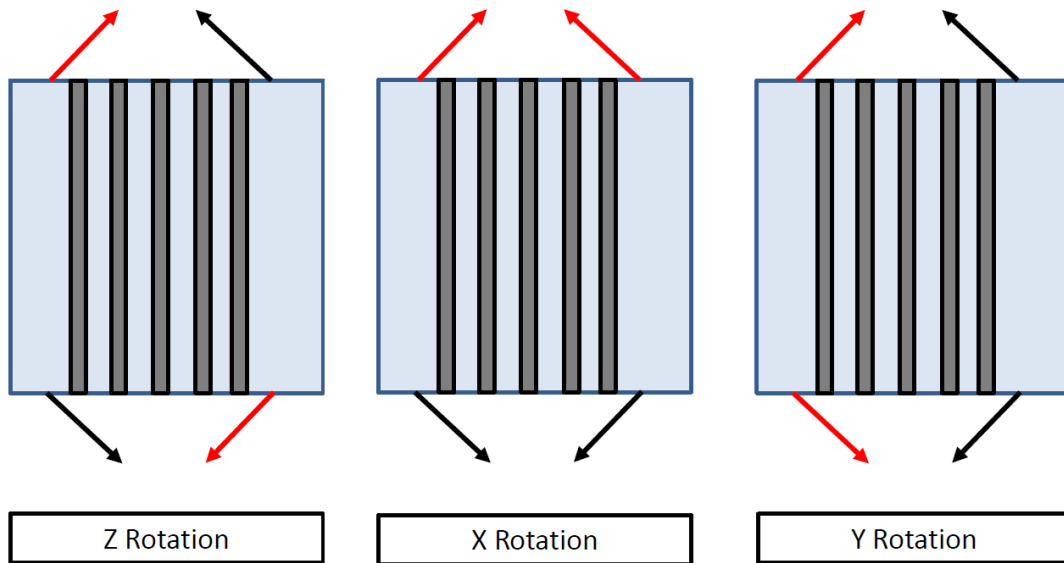


Figure 3.5: Different valve combinations for different maneuvers

firing through different combinations of pairs of nozzles will create a torque on the spacecraft as seen in Figure 3.5; firing through the “opposite” pair of nozzles will create an opposing torque to stop the rotation.

The thruster is filled via a small pre-drilled hole into one of the steel valve manifolds and allows refrigerant to be poured into the main tank and sealed with a screw. In all, the EDU thruster can hold about 100 grams of propellant. Figure 3.6 shows the design and finished assembly of the EDU.

Because the tanks and piping are printed in the plastic manifold, the flow paths of the propellant can be routed in geometries that would not be able to be achieved with traditional steel tubing. Because of this, the piping for each nozzle underwent a flow impedance matching procedure. In this sense, impedance matching means that each path from a valve to the nozzle is the

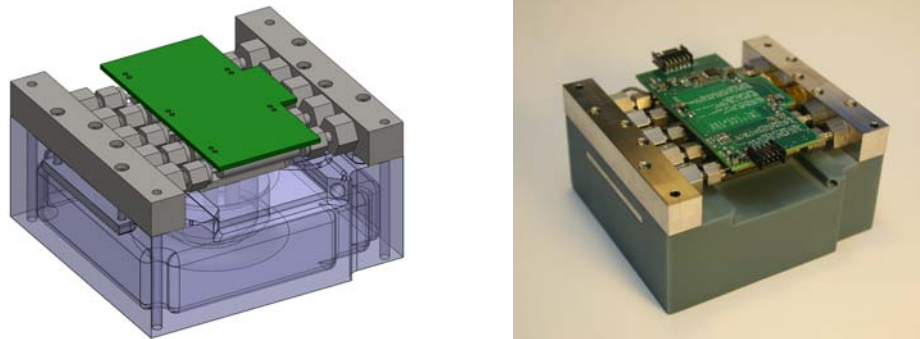


Figure 3.6: The EDU CAD design (left) and the assembled EDU

exact same length and undergoes the same bends and rotations. This was important for the ACS module because one nozzle could be paired with one of the other three to create a rotation around each of the axes. Impedance matching also allows the main command and data handling computer to clock in a single valve open command to ensure that the gas leaves each nozzle at the same time. Figure 3.7 shows a cross section view to highlight the impedance matching bends of the pipes as they go to different locations.

The pressure transducer, thermistor, and heater are connected to an embedded circuit board. The sensors, including the current sense resistor, are connected to an 8-channel 12-bit ADC that is on the CubeSat's I2C bus. A software controlled safety is included on the board to isolate the power bus from the valves. The board uses a shift register to control the valves, safety, and heater; the main command and data handling computer will clock in a byte for a certain valve “on” or “off” configuration and will then push all bytes simultaneously into the output register of the chip. This allows the valve pairs needed for a rotation to be actuated at exactly the same time. The main

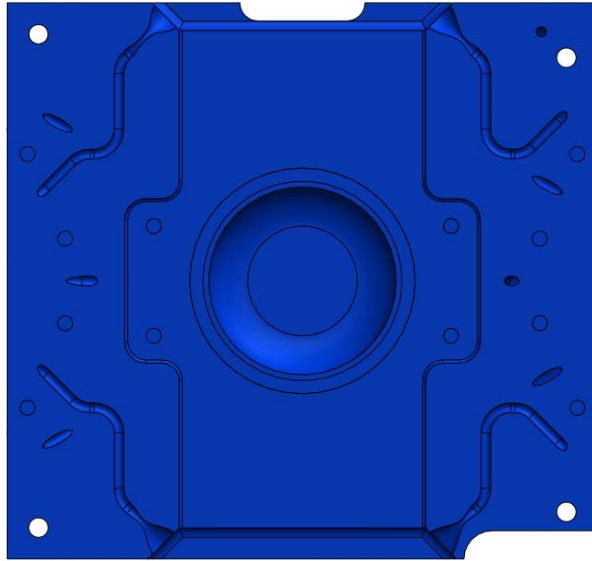


Figure 3.7: Impedance matched piping shown on an EDU cross-section

computer controls the valve timing and will clock in a second byte to close the valves.

The EDU was designed and built in the Spring of 2013 and then transported out to JPL for testing in a thermal vacuum chamber over the Summer. Over the ten weeks in California, several issues were noticed with the EDU. First, the filling port passes through the steel manifold and has no relief port to allow the air currently in the tank to escape. This results in air bubbling back up the filling hole and causes the refrigerant to vaporize before it can enter the main tank. The quick-fix solution is to remove the steel valve manifold and pour the propellant directly into the plastic manifold before quickly reseating the valves. Fortunately, filling the EDU once loads enough propellant for several weeks of testing with that unit.

Beyond the plastic, the EDU is also primarily constructed out of stainless steel to match the material used on the valves. However, INSPIRE's science grade magnetometer has potential measurement interference issues with any steel components. As a result, brass pieces were required for future thruster iterations. The EDU also has a small leak on the expansion tank seal because of an incorrectly sized o-ring and the controlling circuit board has some voltage-level interface issues with the main INSPIRE computer. The thruster also lacks a hardware safety to prevent the thruster from inadvertently firing. The required modifications between the EDU and flight units were significant enough that it was considered too risky to have the flight units be the first test implementation of the new components, including new brass fittings, a closed loop filling system, and upgraded electronics. As a result, the Flight Technology Test (FTT) thruster was created as the next iteration of the design.

3.2.2 FTT Design

The FTT design began in the Fall of 2013 based on the issues and improvements seen with the EDU design. As the overall configuration of the INSPIRE CubeSats matured, the volume allocated to the ACS increased to 0.7U at the end of the summer. This increased the volume available to both the main and expansion tanks and allowed the INSPIRE to carry more propellant. The nozzles on the FTT remain in a similar, 45° configuration to the EDU but are placed closer to the center mass of the satellite to achieve smaller actuation torques. All four nozzles are also canted upward at a 20° angle and

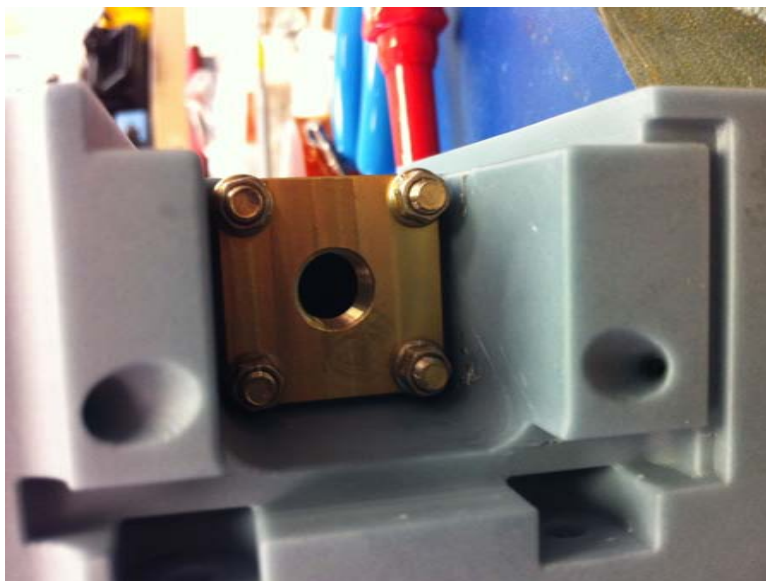


Figure 3.8: Angled and canted 3D printed FTT thruster nozzles

are shown in Figure 3.8. This enables the INSPIRE CubeSats to achieve small ΔV maneuvers by firing through all four nozzles simultaneously. This feature makes the CG ACS system a 4-DOF unit, though the systems are optimally configured for attitude control.

Because of the filling challenges on the EDU, the FTT incorporated a closed-loop filling and draining system that isolated the propellant from the spacecraft during loading. This system would allow the propellant to be loaded into the ACS system while the CubeSats are stored in the P-POD units before launch. A schrader-style valve is mounted on the thruster to allow for two-way flow between the main tank and the ground support equipment and is shown in Figure 3.9. Because the valve is bidirectional, it allows the room air in the main tank to be removed before loading, the propellant to flow in, and if necessary, the propellant to be removed for storage.

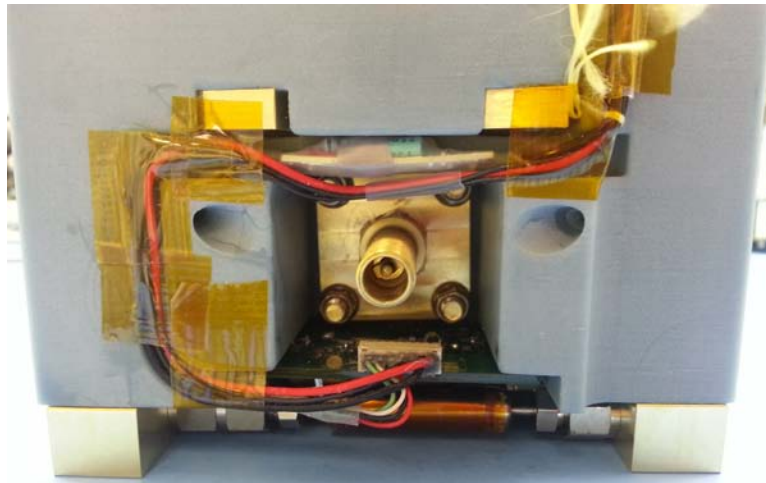


Figure 3.9: The FTT fill and drain valves

The FTT also includes inline filters on each of the valves to prevent particulate from damaging each valve's elastomer seals. Snubber circuitry is included on each valve; since the valves are solenoids, they essentially behave like inductors. The snubber circuitry prevents any power still in the solenoid to be dissipated after the valve has been turned off from the main power bus. The embedded circuit board also includes three safeties: one safety controls the power to the logic components on the thruster and is directly connected to the main computer. A second, hardware safety requires a constant pulse from the main computer and will close all valves if the main computer fails to ping the thruster. The third safety is controlled through the shift register and isolates the power line from the valves. All of these components are shown in Figure 3.10.

Assembly of the FTT was completed in November of 2013 and thrust

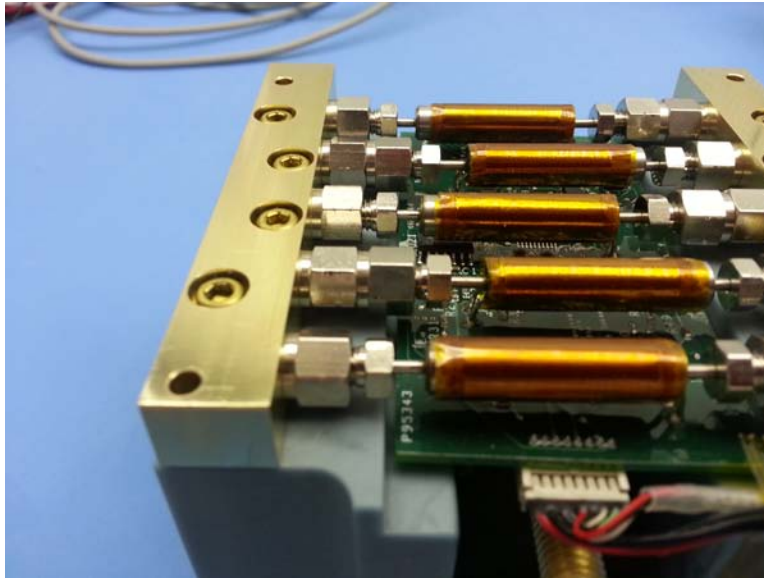


Figure 3.10: FTT fittings, filters, and controlling electronics

determination testing began with the new unit. The unit performed well and indicated that the new brass fittings, filters, and improved circuit board would work for the flight units. However, the increased complexity from the inclusion of the filling port hardware required a more complex plastic manifold than had been designed before. As a result, the manufacturer had more difficulty creating the FTT plastic manifold compared to the EDU or the Bevo-2 plastic; the first printing of the FTT plastic had two leaks within the plastic. From this point, the TSL worked with the manufacturer to optimize the plastic design based on the manufacturing process limitations for Bluestone. Three plastic manifolds were ordered for the flight build, including one to replace the leaking manifold on the FTT.

3.2.3 The Flight Units

The flight units are identical to the FTT initial design apart from a slight internal modification to the interior of the plastic manifold to fix the leak issues. They were built in January of 2014 and are named Castor and Pollux, after the twin brothers that make up the constellation Gemini in Greek and Roman mythology. The two units are identical and are shown in Figure 3.11. The plastic manifold interiors were cleaned and scrubbed with ethanol twenty times to remove any remaining resin or plastic from the printing process. The expansion tank sensor assembly and valve manifolds were secured with a special thread locking compound to prevent fluid leaks. The ACS units were each checked for electrical and mechanical functionality in a clean room environment. Each unit was then loaded with a small amount of propellant, massed, and placed individually into the vacuum chamber. After this, the units were placed under a high vacuum ($5 \cdot 10^{-6}$ torr) for nearly a day then removed and massed again. Neither unit showed any mass difference verifying that the units did not leak at a measurable rate. Each unit was then thrust tested out of all four nozzles to compare the thrust differences between each nozzle. No significant differences were detected between the nozzles within each manifold nor between the two units.

3.2.4 Filling and Ground Support Equipment

Creating a closed-loop filling system for the INSPIRE thrusters was one of the most challenging tasks in the design of the thrusters; there was already past experience with the plastic, valves, and refrigerant and the sensors were

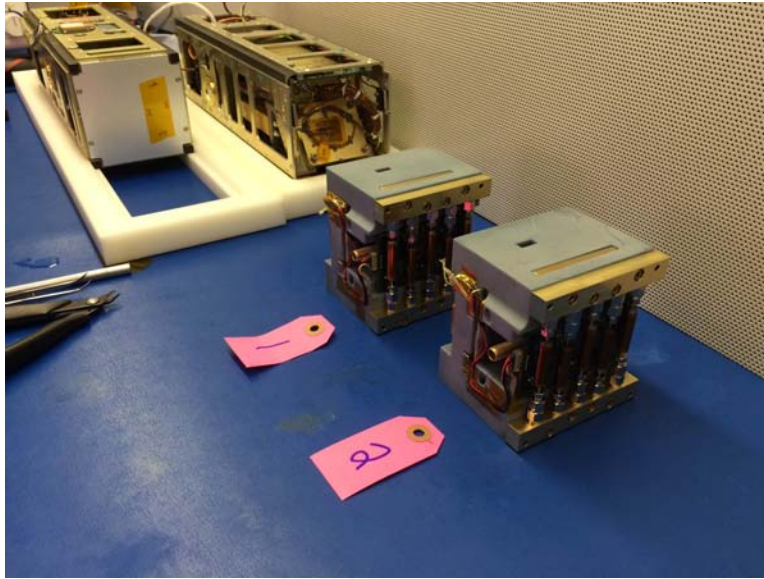


Figure 3.11: The flight INSPIRE ACS units (RACE and Bevo-2 in background)

easy to select and integrate. The filling port has to remain closed at-all-times when not connected to the ground support equipment so a bidirectional valve is required. Powered valves are not ideal because of the amount of energy dissipated by the valve when the valves are held open. For example, the Lee Company valves used for the nozzles and tank control consume several watts of power when being held continuously open. This energy is then absorbed by the refrigerant and causes it to flash off and disrupt the filling procedures. The final selection centered around a schrader-style valve mounted in a brass housing that allowed for two way flow. The schrader core is opened when the other half of the disconnect, attached to the ground support equipment, is screwed into the thruster. When the two pieces are detached, the thruster fill port closes and is held shut by the internal pressure. The threading shown on



Figure 3.12: Fill and drain valve for the INSPIRE flight units [25]

the fill valve in Figure 3.12 is important because it allows a threaded cap to be attached to prevent any small leaks.

A vacuum filling technique is used because the FTT and flight units require a closed loop filling system. Kapton tape is placed over each of the four nozzles and a segment of ground support hose is connected to both a vacuum pump and a cylinder of R236. Each arm of this assembly is isolated with a valve. The small, portable vacuum pump, capable of pulling $25\text{in} - \text{Hg}$, evacuates air from the thruster and tubing harness assembly. Because the solenoid valves open under reverse pressure, this method evacuates the air from both the main tank and expansion tank. The tape over the nozzles prevents the vacuum pump from pulling room air into the unit. After about ten minutes of pulling, the vacuum pump line valve is closed, leaving the system at a vacuum. Figure 3.13 shows the FTT connected to the tubing harness.

The refrigerant tank, which is placed several feet above the thruster on a stand, is opened. The vacuum in the harness and thruster unit pulls the



Figure 3.13: Interface between the filling equipment and the thruster

refrigerant into the plastic manifold. However, because of the nature of the refrigerant, the R236 quickly settles into a saturated state within the thruster volume. In all, the initial in-rush of propellant only loads about 30g of the total 180g. From here, because the ground support tubing and tank are full of liquid and are above the thruster, the downward pressure of the liquid R236 causes the saturated refrigerant in the thruster to recondense. Over the next two to three hours, the liquid fills the thruster leaving the gaseous state in the tubing harness. When the filling process is complete, the valves on the ground support equipment are disconnected and the thruster is sealed by its schrader-style valve.

A special piece of plastic was ordered to test the filling process and procedures. Instead of the Accura Bluestone, an identical manifold was printed out of a clear plastic that allowed the main tank fluid level to be observed during filling. A flight-like fill valve and o-ring seal was secured to the filling mockup and the ground support equipment was connected. This mockup

allowed the flight filling procedures to be refined while providing a helpful insight into the speed at which the thruster tank filled. Additionally, this clear piece of plastic helped act as a leak verification test for the fill port; after being successfully filled multiple times, the tank was filled again and left to rest on the shelf. Over the next six months, the o-ring seal and fill valve showed less than $0.1g$ loss of mass.

Chapter 4 talks about another element of the ground support equipment, the thrust determination stand and vacuum chamber environment.

Chapter 4

Description of Test Equipment

The characterization of the INSPIRE ACS units focused on determining the thrust under different thermal conditions. With knowledge of the mass flow rate, valve timings, and temperature and pressure conditions within the thruster's expansion tank, collected thrust data is used to determine metrics such as minimum impulse bit, specific impulse, and the relationship between the expansion tank pressure to thrust. Two versions of a thrust determination stand were built; a ballistic pendulum stand was used to test the EDU and a more upgraded, digital version was used to characterize the FTT and flight units.

4.1 Approach and Methodology

The CG thrusters produce thrust on the order of tens of millinewtons. To effectively measure forces in this range, the thruster units are tested in the TSL's vacuum chamber to simulate the conditions of space. Some commercial force/pressure sensors exist that can accurately measure forces in this range, though they were generally too expensive to be considered for the scope of this research. Additionally, the flow exiting the nozzles is approximated as a growing cone. With the time constraints to characterize the units, it was

deemed too difficult to integrate a setup where a millinewton-range force sensor could effectively measure the entire thrust generated. This led to the use of a simple and tested ballistic pendulum design.

The ballistic pendulum is proven method to measure thrust using displacements rather than fixed sensors. For testing at the TSL, the thruster is secured to the vacuum chamber floor and the ballistic pendulum end is hung vertically in front of a single nozzle. When the propellant is expelled out of that nozzle, the pendulum displaces a certain amount based on the total impulse generated by the CG unit. This displacement can be measured as a horizontal or vertical linear displacement, or as a maximum rotation from the vertical direction. Both of these methods allow the impulse to be determined either through energy and momentum methods or by numerically integrating the motion back to the initial conditions [14]. The limitation of this method is that the thrust is assumed to be nearly an impulse. As the commanded firings are commanded to be longer in duration, such as a $15ms$ firing, the pendulum has started moving away from the thruster before the propellant has finished being expelled. As such, longer duration pulses are measured to have a slightly smaller thrust with the same initial conditions. Overall, a linear relationship with a slight downward slope is seen as the valve pulses become longer.

4.2 The Vacuum Chamber Setup

The Texas Spacecraft Laboratory is fortunate to have a microtorr-level vacuum chamber for testing of complete 3U CubeSats or specific components. The chamber has an interior 24" cube volume with numerous passthroughs



Figure 4.1: The TSL's microtorr vacuum chamber

for electrical components and thermistors. The vacuum chamber is shown in Figure 4.1. The chamber is able to reach a relatively high vacuum of $5 \cdot 10^{-5}$ within 15 minutes of running and can achieve a maximum vacuum of $2 \cdot 10^{-6}$ after about a day of continuous vacuuming. The chamber features a cold-trap filled with liquid nitrogen that is used to capture any gas from the chamber. This is especially useful for thruster testing so that the refrigerant propellant can be quickly removed between tests. In practice, the chamber only needed four to five seconds to pull the pressure down to starting levels after a pulse was fired from the thruster. This meant a full round of testing of 1250 pulses could be finished in about six hours. A large, 20-pin harness was assembled to power and control the thruster as well as interface with the rotary encoder on the test stand.

The vacuum chamber has not been outfitted with a formal thermal

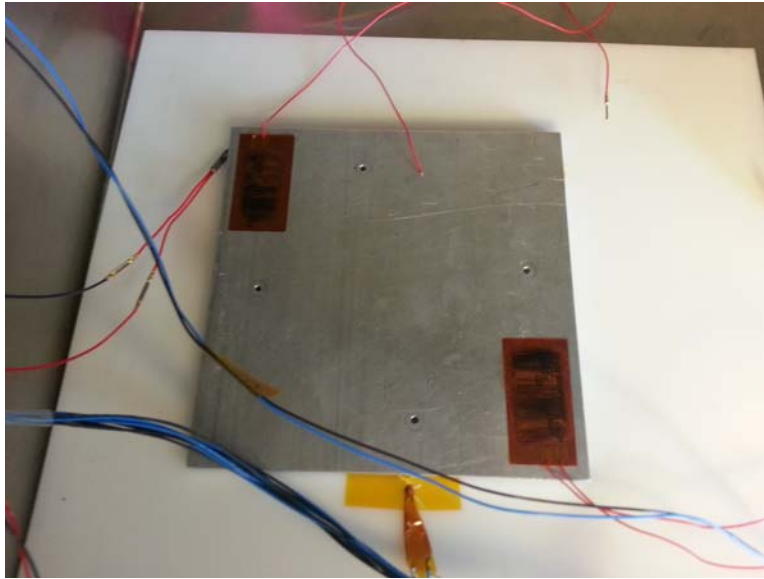


Figure 4.2: The heating plate for the vacuum chamber

vacuum system seen at larger institutions. However, a simple and removable heating plate has been designed for the chamber. Kapton heaters are affixed to a steel plate within the chamber. The chamber is separated from the chamber walls by a slab of half inch thick acetal plastic. The Kapton heaters are connected to an external power supply; depending on the voltage applied to the heaters, they will go to different temperatures. The steel plate is large enough for the thruster to sit on and is shown in Figure 4.2. Five, numbered thermistors can be placed at any point in the chamber as needed by the test. In practice, if an object is being heated, the heaters are turned on 24 hours before a test to allow for conditions to reach a steady state. An additional 16-pin harness controlled the heaters and connected the thermistors back to the supporting computer.

4.3 Test Stands

Two test stands were built to characterize all of the ACS units built. The EDU test stand was created for the summer testing of the EDU at JPL. An improved stand was built to characterize both the FTT and flight units.

4.3.1 EDU Test Stand

The EDU stand was based off the heritage from testing the Bevo-2 thruster, where a lightweight aluminum cup suspended by lightweight fishing line was positioned in front of the nozzle. When the Bevo-2 thruster was fired, a webcam installed in the vacuum chamber recorded a video of the displacement that was viewed in post-processing to measure the maximum displacement angle. Because the INSPIRE EDU was predicted to generate a smaller force than the Bevo-2 unit, a lighter piece of aluminum (about $2.4g$) was used as the pendulum mass. The center of mass of the pendulum was positioned directly in front of the nozzle and was large enough to ensure that the whole thrust cone would impact the aluminum.

The EDU test stand required a webcam to be positioned directly above the thruster and pendulum. Beneath the thruster, a “checkerboard” pattern was printed on a piece of paper. The checkerboard had a $0.1in$ spacing with alternating black and white squares. During the firings of the EDU unit, the webcam recorded a series of displacements of the pendulum. The video was then later watched and the horizontal displacement was determined using the checkerboard pattern as a distance reference. This method was a quick and simple way to determine the thrust, but relied on a person to watch each video

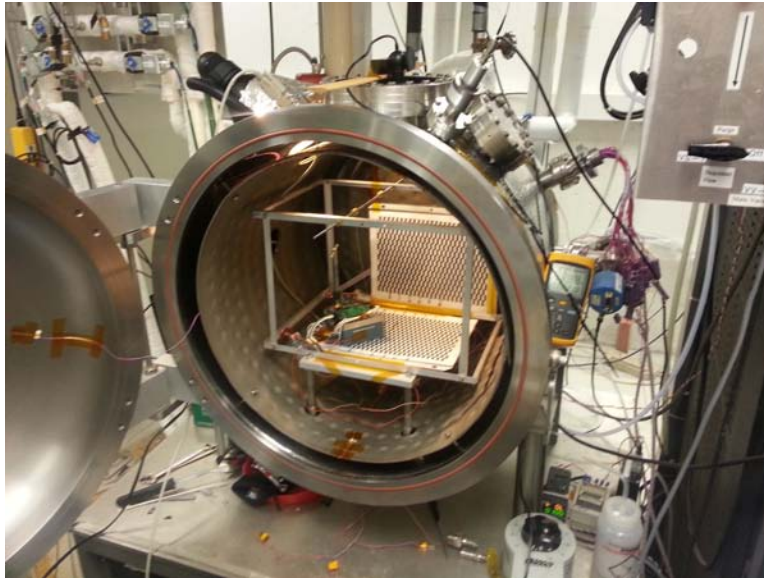


Figure 4.3: The test chamber and stand for the EDU

and determine the maximum displacement manually. Additionally, the fishing line that was used to suspend the pendulum mass exhibited some torsional rotation during the firings. While this test stand did give useful preliminary insight into how the INSPIRE ACS systems would behave, the need for a revised, more accurate, and automatic test stand was needed to characterize the flight units. Figure 4.3 shows the vacuum chamber and test stand used with the EDU during the summer testing.

4.3.2 Flight Collection Stand

The FTT and flight collection stand is designed to accurately measure the very small thrust pulses. A 10 – *bit* rotary encoder is connected to a rigid pendulum constructed out of garolite, a lightweight and vacuum compatible composite. The garolite pendulum is balanced to maximize the total angle the

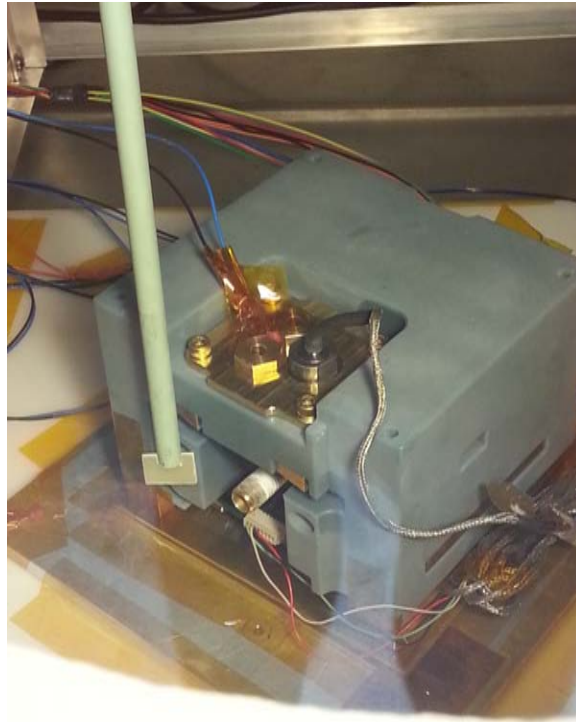


Figure 4.4: The FTT with the test stand in the vacuum chamber

pendulum will sweep through for very small impulses while also minimizing the deflection of the pendulum during the actual thruster pulse. With the inclusion of the rotary encoder, a new set of challenges were introduced in measuring the pendulum's deflection; the rotary encoder depends on lubricated bearings to rotate, and once the lubricant began to break down in a hard vacuum, there were measurable frictional losses during the pendulum rotation. This pendulum is shown positioned with the FTT in Figure 4.4.

Characterizing and understanding the frictional losses improves the accuracy of the thrust measurement and is important to understanding the energy balance of the pendulum's motion. The encoder has a finite step size

(approximately 0.35°) so very small deflections are not afforded the same “resolution” as large deflections. Minimizing the deflection during the pulse improves the impulse assumption because a slower swinging pendulum will see fewer frictional loss effects. In the end, a heavy but well-balanced pendulum is included that will swing slowly because of its high moment of inertia and swing further because of the counterweight. The pendulum is secured to the rotary encoder and the rotary encoder is mounted on a test stand that can be adjusted to match the geometry of the thruster below it. The encoder’s analog output is connected through an analog to digital converter and interfaced with LabView. The LabView software runs independently of the CG thruster firing software and samples the rotary encoder at $5kHz$ and exports the data as a file to be processed later.

4.4 LabView Controllers

The LabView software by National Instruments is used to run the data collection scripts for the temperature and pendulum deflection. Custom VI’s were written to interface with the TSL’s LabView data acquisition units. The temperature VI simply records temperature over time from each of the thermistors to confirm that the units are at a steady state temperature when being tested. The deflection collection VI allows for some automation to be taken care of by the software. For example, the program will read in how many runs will be measured from the thruster, creates a unique file name for each run and saves the data, and allows the user to pre-program in a wait period for the vacuum chamber to remove propellant from the chamber before the following

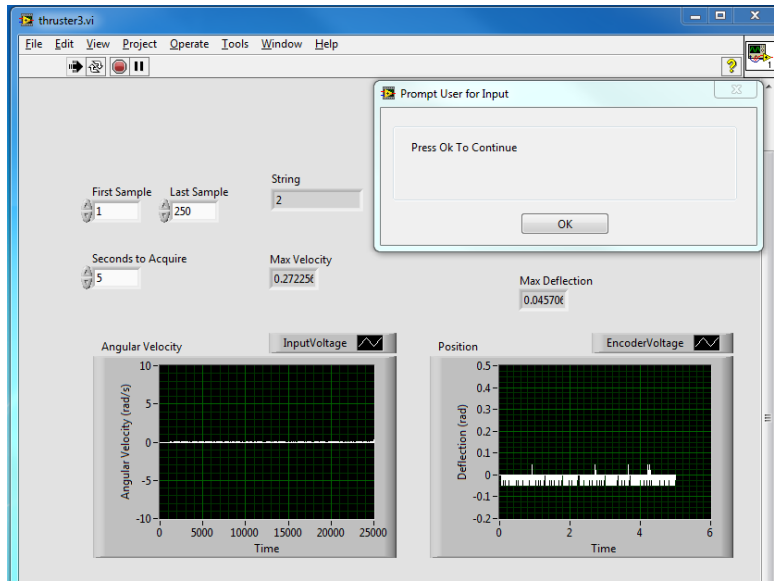


Figure 4.5: The LabView VI to measure pendulum deflection

tests. The VI also provides visual validation that a pulse has been recorded by showing the deflection waveform. Additionally, because the thruster is commanded through a separate Linux system, it waits for a user confirmation between tests to make sure the VI is running when the thruster is actuating. A screenshot of the deflection VI is shown in Figure 4.5.

4.5 Calibration Methodology

The lubrication within the rotary encoder began to break down under the high vacuum conditions almost immediately; the increasing friction was noticed on the first test run with the new test stand. After continued experimentation, the encoder was observed to reach a point where the lubrication did not continue to break down and the friction was predictable.

This highlighted the need to calibrate the response of the stand since it was no longer assumed to be friction free. This calibration was done using using a step response function.

For calibration, the stand was zeroed at the vertical position. The pendulum was manually deflected to an angle of 15° and the deflection recorded with LabView at $5kHz$ as it swung through the zero position. This waveform is treated as the step response of a second-order dynamic system and no higher order loss terms are assumed to exist. The step response is a function of the moment of inertia of the pendulum, the center-of-mass offset from the fulcrum, and the frictional losses of the pendulum. The center of mass offset and total mass were measured using calipers and a digital scale so only the moment of inertia needed to be determined. A least squares method was used to fit the step response function to the first two full oscillations of the pendulum and determine the inertia.

To perform this fit, the pendulum is modeled as a second-order dynamic system, described by the differential equation:

$$I\ddot{\theta} + c\dot{\theta} + \frac{g}{x_{cg}}\theta = 0$$

For simplicity, we can define the following quantities to represent the equation in the standard second order ODE form.

$$\omega_n^2 = \frac{g}{I \cdot x_{cg}}$$

$$\zeta = c \sqrt{\frac{x_{cg}}{I \cdot g}}$$

This gives the equation for a general step response [26]:

$$x(t) = \frac{1}{\omega_n^2} \left[1 - e^{-\sigma t} \left(\cos \omega_d t + \frac{\zeta}{\sqrt{1 - \zeta^2}} \sin \omega_d t \right) \right]$$

The pendulum's displacement waveform was recorded and fit to this predicted curve to estimate the effect of the friction. This fit gave a natural frequency of $26.67 \frac{rad}{s}$. The center of mass offset has already been measured as $27.4mm$ and using the calculated value of natural frequency and known value of gravity the moment of inertia was determined to be $1.98kg \cdot m^2$.

Chapter 5

Thrust Determination and Analysis

Using the flight collection test, thrust determination tests were run on the FTT thruster. These tests were conducted after the flight units had been delivered and the original, leaking plastic manifold for the FTT had been replaced with a manifold identical to the flight units. The tests focused on characterizing the relationship between thrust and temperature, as well as resolving the minimum impulse bit and specific impulse. This chapter includes the testing methodology, results, challenges faced during testing, and concludes with an analysis of the results.

5.1 Collection Methods

With the test stand, LabView, and vacuum chamber set up, additional hardware was setup to control the actual thruster commands and data recording. A few test runs were done before the main data collection period to make sure the software and hardware worked as expected and to understand how long each test would take when organizing a testing schedule. Some challenges with the supporting hardware were seen, but overall did not impact the fidelity of the data.

5.1.1 Setup

A total of eleven trials comprised of 15,000 pulses were run on the FTT unit. Three tests were run at room temperature, with one trial at the saturation pressure and two at lower pressures. Using the thermal heating element in the chamber, four different, heated temperatures were investigated. At each of these temperatures, a trial was done at the determined saturation pressure as well as at a lower pressure. For each temperature run, this lower pressure was chosen to match the saturation pressure at room temperature. The presented tests are delineated by the ADC value reported by the pressure sensor (PADC) - this is the 12 - *bit* analog to digital converter value of the pressure sensor and represents a direct measurement from the expansion tank.

The first test was at room temperature and saturation pressure. 250 firings were collected for ten different times: 1, 2, 3, 4, 5, 6, 8, 10, 12, & 15*ms*. Quick processing of this data showed little variation in the thrust between each of these valve times, so in the interest of total testing time duration, fewer times were tested on subsequent runs; for the remaining ten tests, 250 firings were collected at 1, 2, 4, 6, & 10*ms*.

The thruster drivers are written in C and are executed on a Phytex LPC3250 ARM9 system-on-a-module (SOM) running Linux. This system was chosen because it is the same embedded system used by other TSL missions and provides easy interface to peripherals such as the thruster. This computer also reads the data from the analog to digital converter and exports files for later analysis. While this system works relatively well for running the thruster,

| Heated Run | Heater Voltage (V) | Observed Temperature ($^{\circ}C$) |
|------------|--------------------|--------------------------------------|
| - | Off | 20.6 (Room Temperature) |
| 1 | 5.0 | 26.7 |
| 2 | 6.8 | 29.4 |
| 3 | 8.7 | 32.8 |
| 4 | 10.5 | 38.9 |

Table 5.1: Thermal Test Steady State Temperatures

some challenges were discovered and are discussed in 5.1.3.

Several data elements are collected each time the thruster pulses. The SOM records the commanded valve pulse time, the actual pulse time, and the pressure after the pulse. This data is concatenated into a single timing file for each specific valve timing. The deflection is recorded into an individual file per pulse and logs the deflection angle versus time. This allows the maximum deflection to be calculated within the thrust determination scripts. Temperature is also recorded using LabView and the data is post-processed in MATLAB.

5.1.2 Conditions

For each of the tests, the temperature of the propellant was measured by several thermistors placed around and on the thruster. For each heated test, the heaters were turned on at least 24 hours before testing to allow the temperature to reach a steady state point. Table 5.1 shows the relationship between the heater voltage and the steady state temperature of the propellant.

The thruster measures the pressure within the expansion tank only - there are no sensors in the main tank. The pressure transducer responds linearly to increases in pressure. Though a calibration is provided for each

| Heated Run | Fluid Saturation Pressure (<i>psia</i>) [18] | Observed PADC Value |
|------------|--|---------------------|
| - | 33.96 | 415 |
| 1 | 41.76 | 500 |
| 2 | 45.73 | 535 |
| 3 | 50.87 | 585 |
| 4 | 61.41 | 695 |

Table 5.2: Pressure Transducer Calibration

individual sensor, the transducer was recalibrated using measured temperatures and comparing the PADC values to the saturation pressure read from the R236 data sheet [18]. Saturation conditions were achieved in the expansion tank by allowing the pressure between the main tank and expansion tank to equalize by holding the valve between the two tanks open for multiple seconds. Because of the geometric arrangement of the thruster for ground testing, the piping inlet from the main tank to the expansion tank is on the top face of the main tank. This ensures that only a vapor form of the propellant is transferred between tanks; the main tank remains as a saturated liquid and at saturation pressure. This is not the case on orbit, where the liquid form of the refrigerant will adhere to the walls of the tank. Millisecond-level control of the valve between the two tanks is paired with constant pressure monitoring in the expansion tank in a software loop. This will allow a vapor state to be kept in the expansion tank even in the absence of gravity. Small quantities of liquid can be transferred such that any refrigerant expands into a vapor in the expansion tank. Table 5.2 shows the observed PADC value compared to the saturation pressure of the propellant for the temperature achieved in the heated runs.

Figure 5.1 shows the linear fit of the PADC value to the actual pressure within the expansion tank expected for the measured temperatures. The ADC values show the expected linear relationship expected from the pressure transducer output. The propellant will exist as a pure vapor in any region below the best fit line, a condition that must be met in the expansion tank. This allows the INSPIRE units to sample both the pressure and temperature from the expansion tank and determine the state of the propellant. The actual pressure can be determined by the formula:

$$Pressure = PADC \cdot 0.1 - 7.2$$

In the flight configuration, a look-up table for the temperature ADC value and pressure ADC value will allow the main computer to determine the propellant state and thrust performance for that pressure.

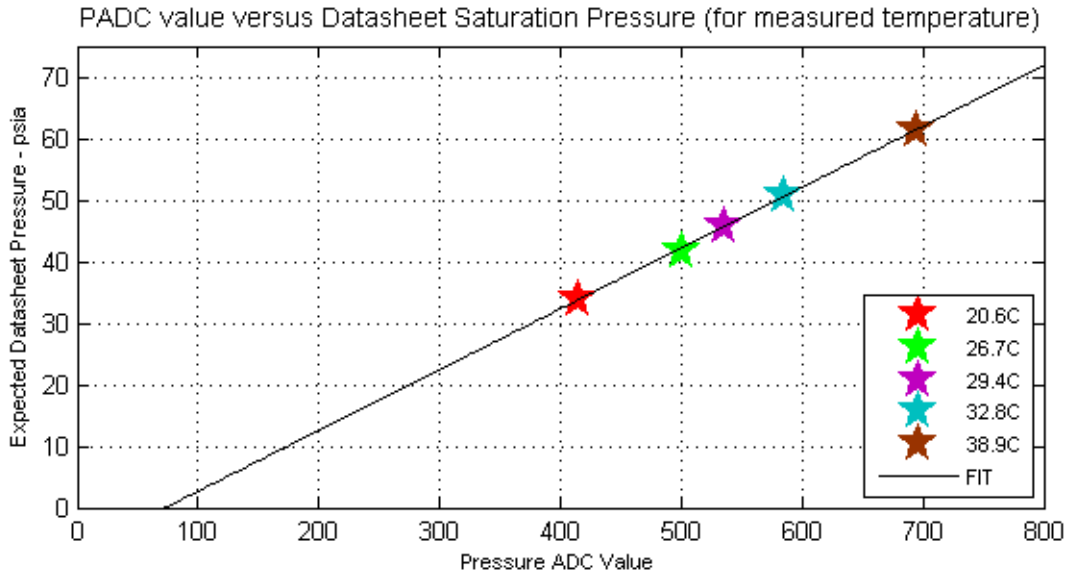


Figure 5.1: Pressure ADC calibration

Another concern was the behavior of the refrigerant versus pressure for the temperatures tested in the vacuum chamber. Over the full range of temperatures R236 can be used for ($-100^{\circ}F - 200^{\circ}F$), the refrigerant pressure shows an exponential relationship in pressure versus temperature. However, as seen in Figure 5.2, the pressure varies nearly linearly with temperature for the temperatures investigated. This is important for fitting the thrust data across temperatures and led to an assumed linear relationship between thrust and pressure.

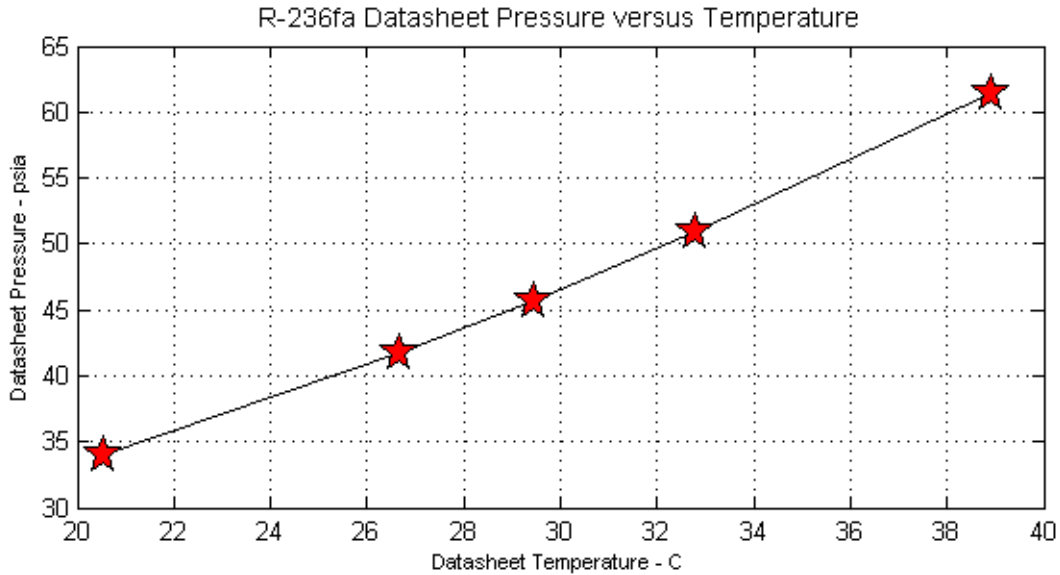


Figure 5.2: Refrigerant Properties in Tested Range [18]

5.1.3 Supporting Hardware Challenges

During the testing of the FTT, some pulses would register as extreme outliers compared to the majority of the data points.. For example, a commanded thrust pulse would cause the SOM to hang without firing the thruster; this happened a maximum of three times per 250 firings and were discarded. Additionally, the thruster unit relies on the microsecond-level clock within Linux to determine the elapsed time between valve open and valve close commands. Between these bytes, a system level sleep command is used. However,

because Linux is not a real time system, the commands were subject to the priorities of the software scheduler.

In practice, the sleep command is extremely effective for sleep times above $10ms$. However, with all of the $1ms$ times, a simple $100\mu s$ error in the actual valve timing changed the thrust by 10%. Figure 5.3 shows three highlighted tests and the observed thrust difference between $1ms$ and $2ms$ tests. These thrust results are expected to be mostly the same, but the $1ms$ timings showed thrusts several times the thrusts measured at $2ms$ and are not physically possible.

Though just three of the eleven tests are shown in Figure 5.3, all tests showed $1ms$ timings that had thrusts much higher than expected, even exceeding the maximum possible thrust as predicted from the isentropic flow equations. Beyond this, the thrust should be equivalent, if not lower than, the thrust from the longer pulses. The reason for this is related to the “ramping up” of the flow through the nozzle. When the solenoid valve opens, the fluid is affected by both the opening and closing motion of the seal. At fast timings near $1ms$, this would potentially create more turbulence in the flow or not allow the flow to reach the full pressure of the expansion tank. Additionally, the post-processing script reads in the impulse from LabView and the actual valve timing from the SOM timing file. The force is calculated by dividing the impulse by the time. Therefore, errors in the time measurement near $1ms$ have large implications on the plotted thrust and affect it as $\frac{1}{x}$. As such, the $1ms$ timings were excluded entirely from the presented plots.

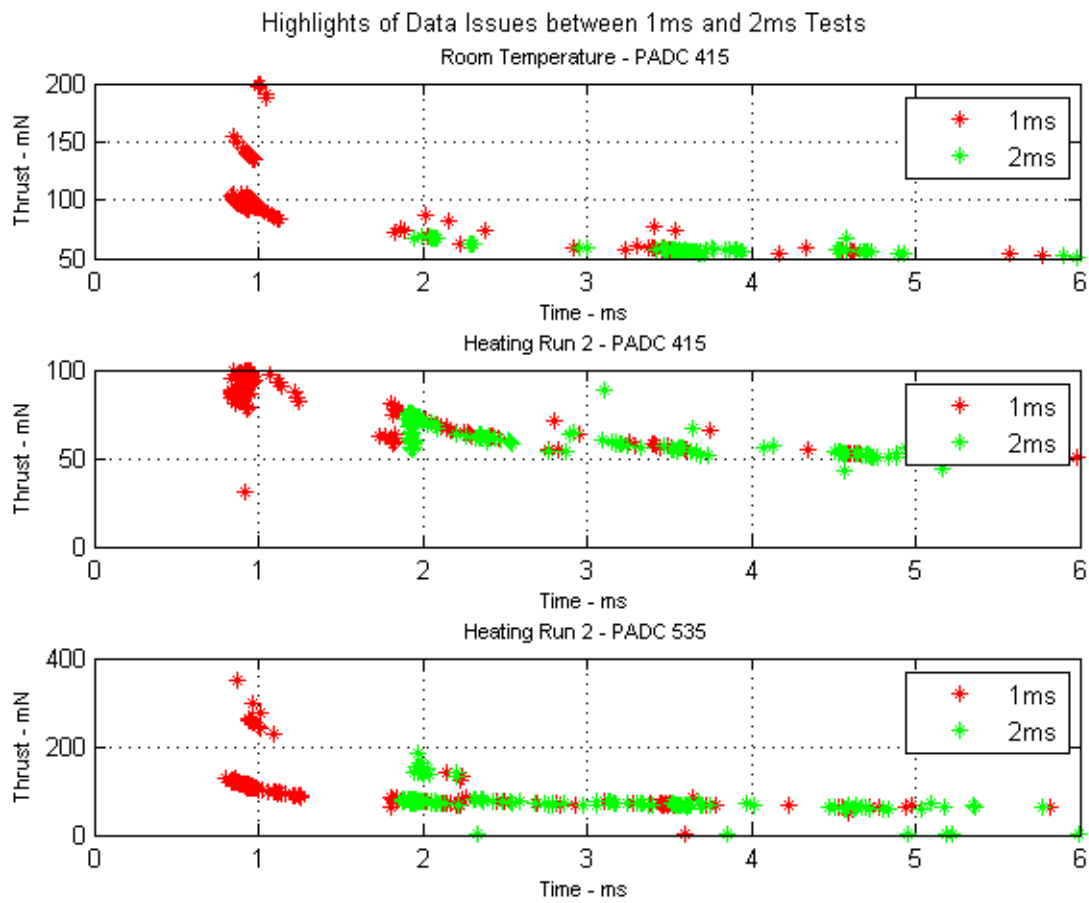


Figure 5.3: Thrust differences based on sample time

The incorrect thrust determination data for the $1ms$ timings does not indicate a problem for the thruster nor the test stand. The shift register embedded on the thruster units is capable of responding to commands on the nanosecond scale, if they are actually issued that fast from the controlling computer. The plotted higher thrusts correspond to the rotary encoder detecting an actual deflection for a longer duration time than was recorded. However, the onboard timing on the selected Linux system does not appear to control nor report accurate timings under $2ms$ because of issues with the scheduler. The INSPIRE systems are flying real-time operating systems and should not see similar issues when commanding the thruster for a specific time.

While the research aimed to deliver the smallest impulse bit, the fastest actuation time claimed by The Lee Company for the valve is a sustained $500Hz$ or $2ms$. The FTT testing could not confirm that the valve could open any faster than this, though single pulses should be able to be faster than $2ms$. This is a topic for a future testing.

5.1.4 Presentation of Data

The presented data has been filtered for presentation. The $1ms$ timings were collected but are not included for the aforementioned reasons. Additionally, extreme outliers were removed to aid with plot scaling and presentation. This includes any zero thrust points, timings beyond the tested range, and extreme obvious outliers. The plots show nearly 1000 pulses each, but the plotted points rarely fall close to the actual commanded valve time; this is still acceptable data.

The Linux system still experienced timing issues between the commanded and actual times. However at and above $2ms$, the reported time more closely matched how long the valve was actually held open; this is in contrast to the $1ms$ time where the reported time was clearly not the correct execution time. Because of the way the data is collected, the individual test is not dependent on the commanded time for each pulse; the system records the actual time the valve is open and is later correlated to the measured impulse from the encoder. For example, if the pulse time was longer than commanded then the measured impulse would likely also be larger and ultimately give the same thrust.

Another trend in the data is the appearance of stripes or striations. This is expected and acceptable. These striations resemble a plot of $y = \frac{1}{x}$ and are related to the finite resolution steps of the rotary encoder. The encoder only has a finite number of steps within the deflection range used for this characterization and the measured impulse is divided by the commanded valve time. Small, $10-$ to $100 - \mu s$ variations in the commanded valve time create this visible striations as the same encoder is divided by slightly different times. Ways to improve the data collection are covered in Chapter 6.

5.1.5 Best Fit Lines

Best fit lines are shown in each of the plots. This linear fit allows the actual thrust produced by the nozzle to be found by looking at the y-intercept value. This method helps analyze the impulse assumption used when working with a ballistic pendulum. As the timings get longer and longer, the

impulse assumption breaks down. Though the times are still very fast, the pendulum moves farther and farther away from the propellant cone as the pulse times increase. Within this time scale, the result is a linear relationship between thrust and pulse duration with a slightly downward slope. This is apparent in all of the plots generated. Additionally, because the $1ms$ times were unusable for calculations, finding the y-intercept of the best fit line is the best approximation of the true thrust generated by each nozzle.

5.2 Thrust Determination Data

The following plots show the filtered thrust measurements with best fit lines. Eleven total plots are presented.

5.2.1 Room Temperature

Three tests were conducted at room temperature, one at the saturation pressure (PADC 415) and two at lower pressures, (PADC 300 and 200).

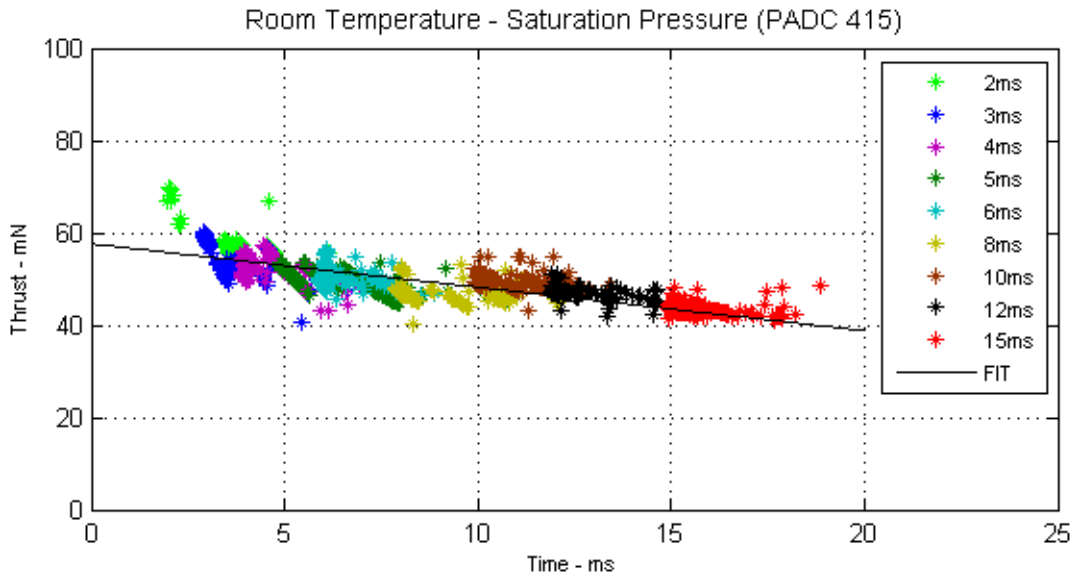


Figure 5.4: Room temperature test at saturation pressure

The fit line shows a generated thrust of $57.6mN$ with an R^2 of 0.627.

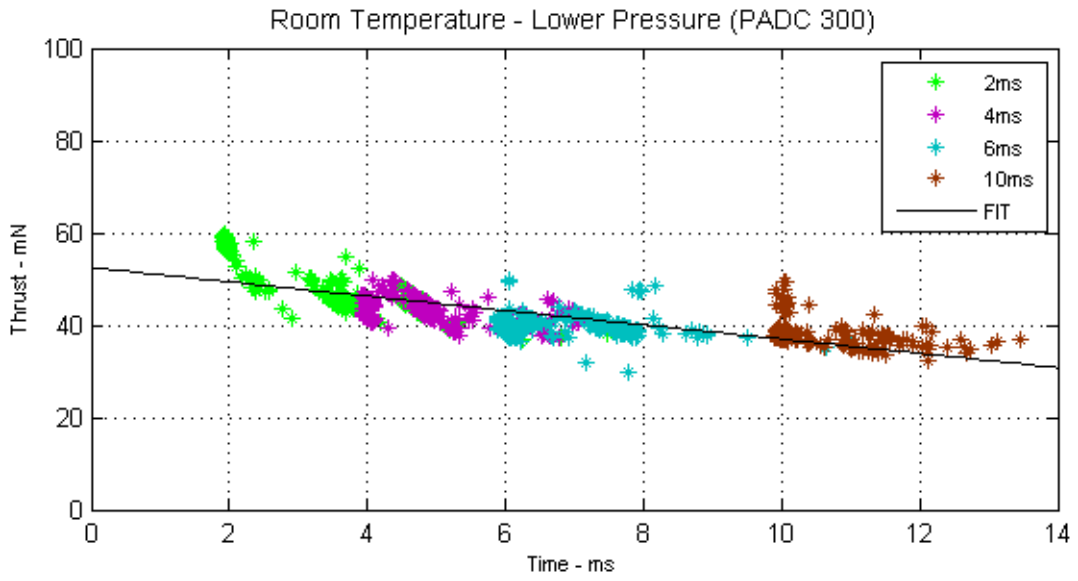


Figure 5.5: Room temperature with the PADC at 300

The fit line shows a generated thrust of $52.4mN$ with an R^2 of 0.576.

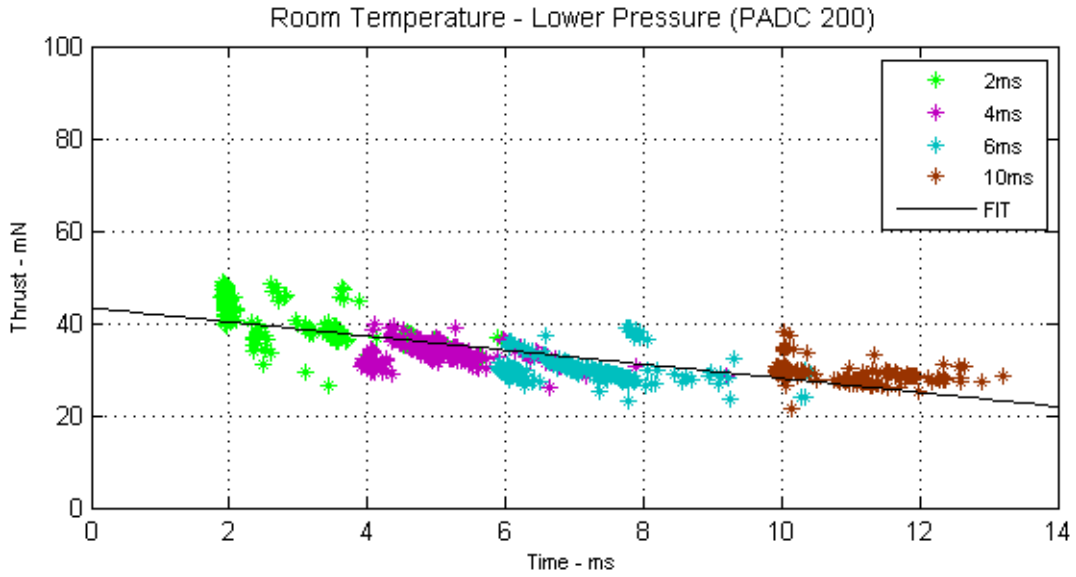


Figure 5.6: Room temperature with PADC at 200

The fit line shows a generated thrust of $43.3mN$ with an R^2 of 0.593.

5.2.2 Heated Tests

Eight tests were conducted at the temperatures listed in Table 5.1. Each test had one run at the room temperature saturation pressure (PADC 415) and an additional run at the saturation pressures listed in Table 5.2.

5.2.2.1 Below Saturation Pressure

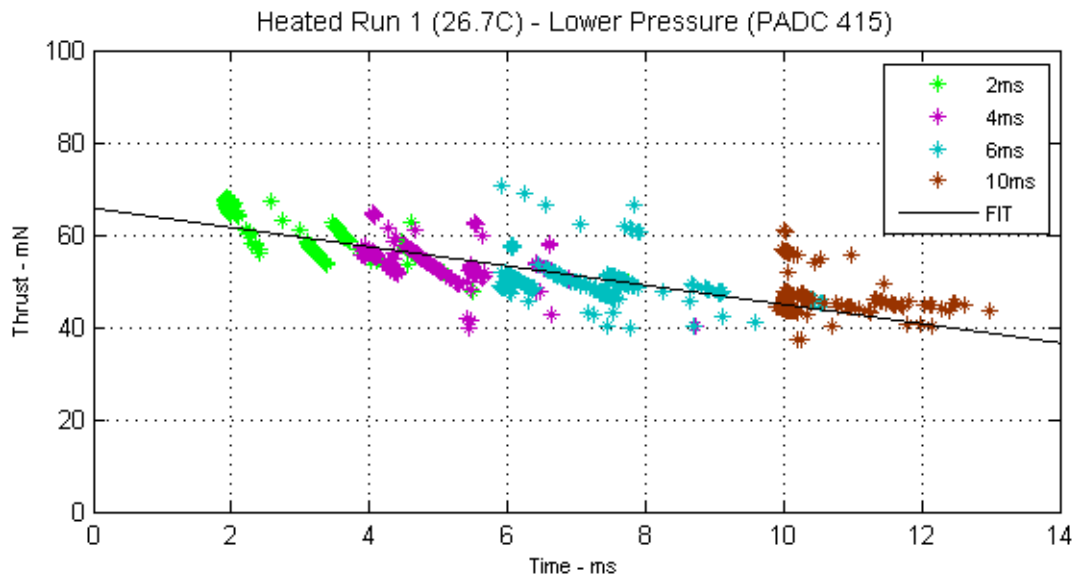
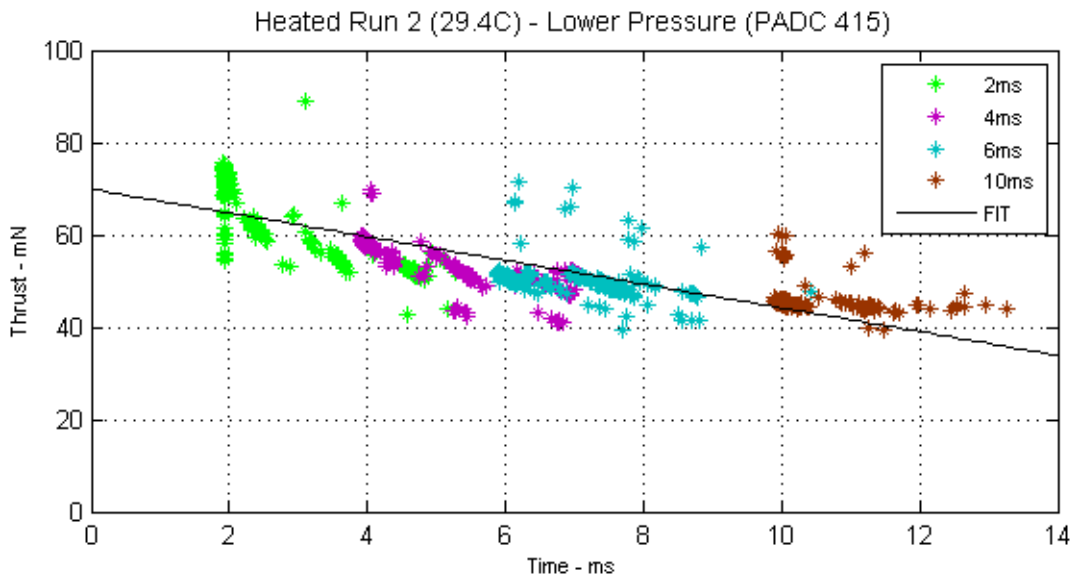


Figure 5.7: Heated run 1 with PADC at 415

The fit line shows a generated thrust of $65.7mN$ with an R^2 of 0.726.



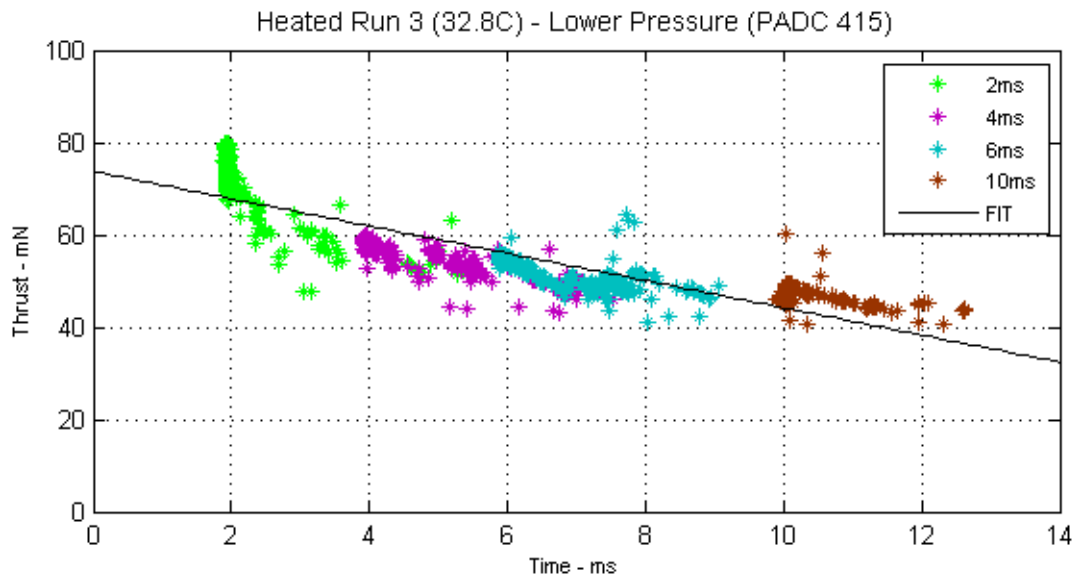


Figure 5.9: Heated run 3 with PADC at 415

The fit line shows a generated thrust of $73.7mN$ with an R^2 of 0.767.

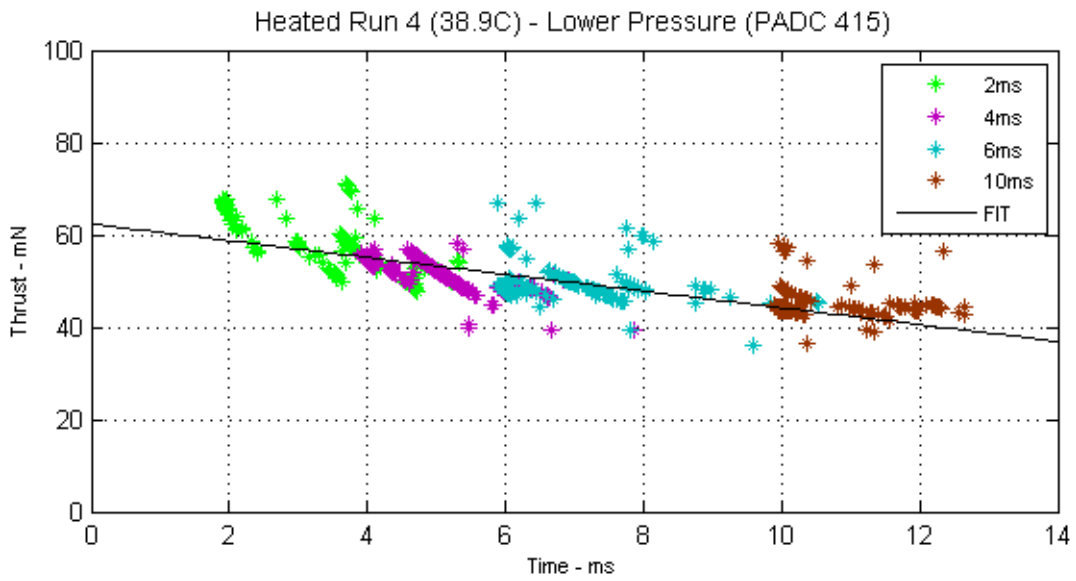


Figure 5.10: Heated run 4 with PADC at 415

The fit line shows a generated thrust of $62.3mN$ with an R^2 of 0.628.

5.2.2.2 At Saturation Pressure

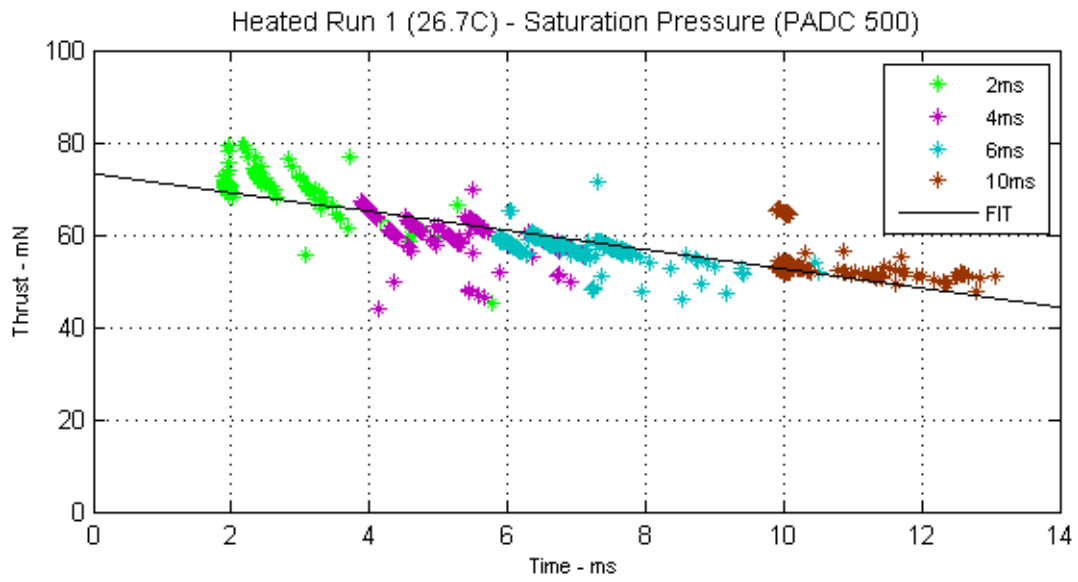


Figure 5.11: Heated run 1 at saturation pressure

The fit line shows a generated thrust of $73.3mN$ with an R^2 of 0.796.

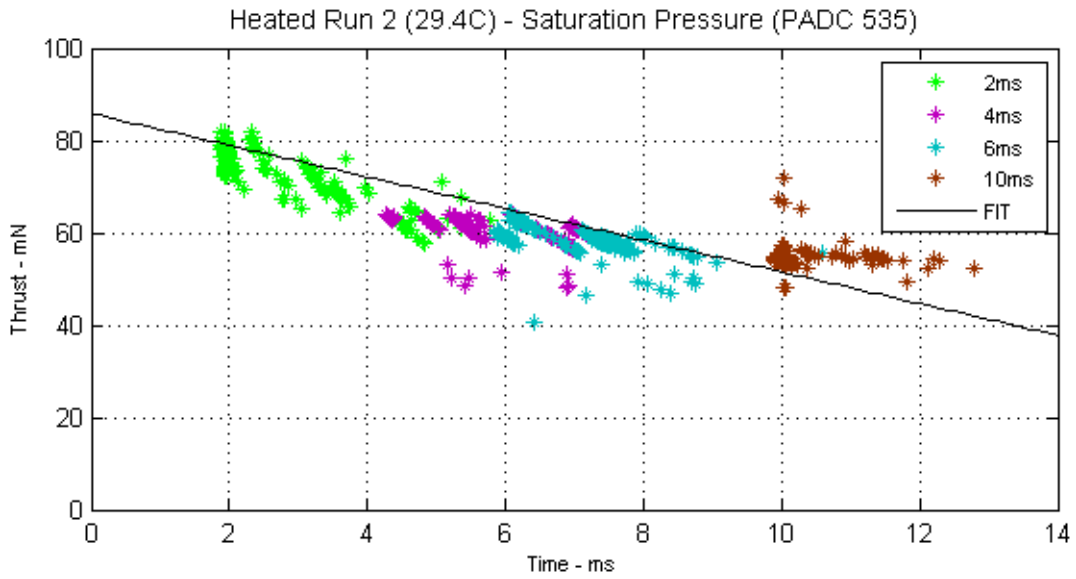


Figure 5.12: Heated run 2 at saturation pressure

The fit line shows a generated thrust of $85.8mN$ with an R^2 of 0.470.

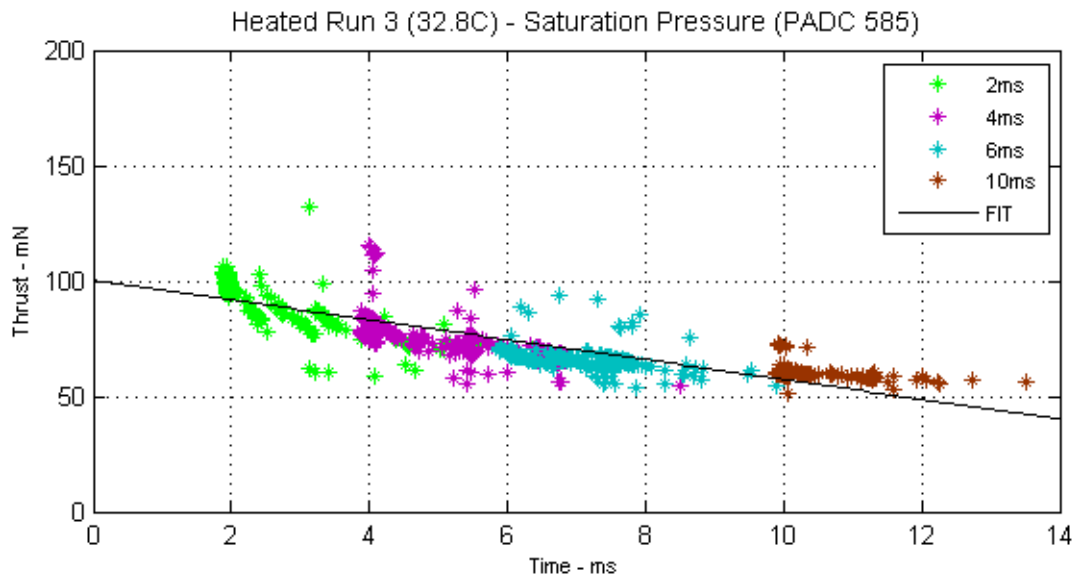


Figure 5.13: Heated run 3 at saturation pressure

The fit line shows a generated thrust of $100.4mN$ with an R^2 of 0.772.

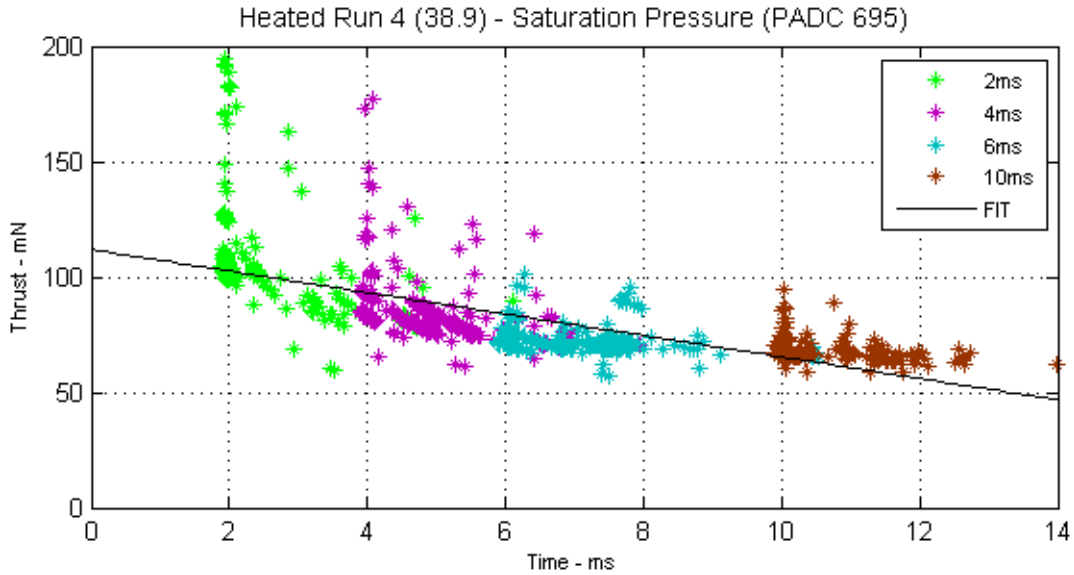


Figure 5.14: Heated run 4 at saturation pressure

The fit line shows a generated thrust of 111.8mN with an R^2 of 0.510.

5.2.3 Summary of Results

Table 5.3 shows a summary of the eleven runs.

5.3 Combined Results

To establish a relationship to describe the thrust, all of the data sets were analyzed together. As expected, there is a trend that the thrust increases as the pressure increases. In the case of the refrigerant propellant, the satu-

| Test Description | Thrust (mN) | Correlation |
|------------------------|-----------------|-------------|
| Room temperature (415) | 57.6 | 0.627 |
| Room temperature (300) | 52.4 | 0.576 |
| Room temperature (200) | 43.3 | 0.593 |
| Heated 1 (415) | 56.7 | 0.762 |
| Heated 1 (500) | 73.3 | 0.796 |
| Heated 2 (415) | 69.9 | 0.695 |
| Heated 2 (535) | 85.8 | 0.470 |
| Heated 3 (415) | 73.7 | 0.767 |
| Heated 3 (585) | 100.4 | 0.772 |
| Heated 4 (415) | 62.3 | 0.628 |
| Heated 4 (695) | 111.8 | 0.510 |

Table 5.3: Summary of testing results for each run

ration pressure is based only off of the temperature of the propellant. With knowledge of the spacecraft temperature, expansion tank temperature, and expansion tank pressure, the INSPIRE attitude control algorithms can determine the correct pressure in the expansion tank to deliver the desired thrust force. Beyond the thrust, the specific impulse and minimum impulse bit were measured at room temperature conditions.

5.3.1 Thrust Determination

The five tests conducted at PADC 415 were combined onto a single plot and fitted, shown below in Figure 5.15. The data for the five different temperatures at the same pressure shows encouraging results; the thrust is consistent for a given pressure and is independent of temperature within the temperatures tested.

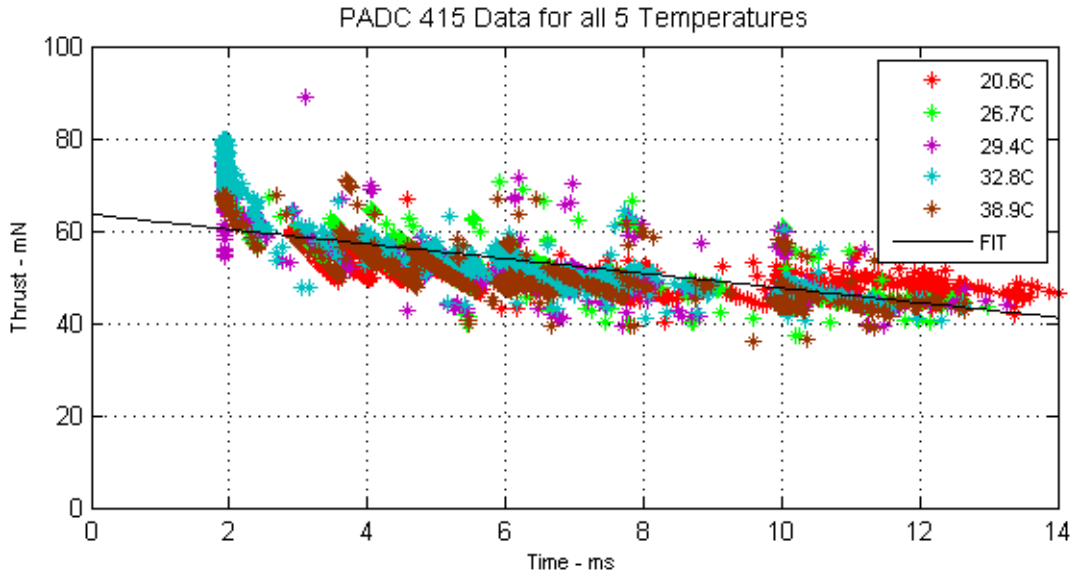


Figure 5.15: All data for PADC 415

As discussed previously, the data shows a linear relationship between valve timing and thrust. The timing errors near the $2ms$ mark make certain trials stand out more than others. This is still a result of the microsecond error in the actual valve timing that is divided into the measured impulse. For all of the PADC 415 values, the average generated thrust is $63.5mN$ with an R^2 of 0.510.

Using the predicted thrusts for each of the tests (and the overall averaged PADC 415 value), a fit was done to correlate the expansion tank pressure to the generated thrust. This is shown in Figure 5.16.

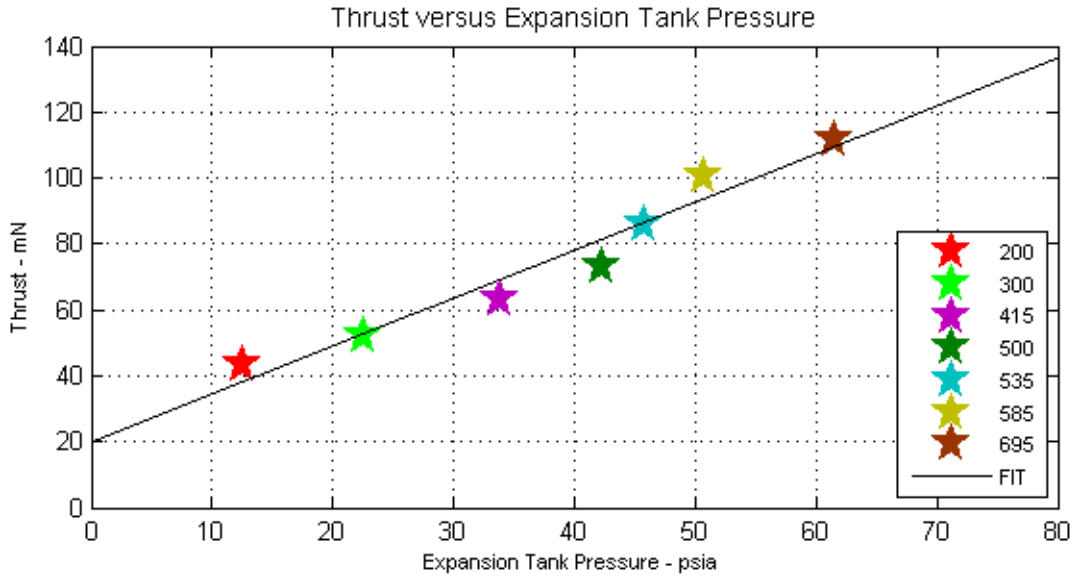


Figure 5.16: Thrust compared to expansion tank pressure

The thrust data shows a rough linear relationship between the data with an R^2 of 0.953. This matches the predictions we made in Subsection 5.1.2 about the profile of the propellant's pressure versus temperature. This results in the relationships seen below:

$$Thrust (mN) = Pressure (psia) \cdot 1.46 + 19.91$$

This can be related algebraically to the PADC value.

$$\boxed{Thrust (mN) = PADC \cdot 0.144 + 9.41} \quad (5.1)$$

Instead of having zero thrust when the pressure is zero, the equation shows a *y-intercept* value. This is expected because the thrust is expected to show some form of a “ramp up curve” from the origin as the pressure difference increases. From this equation, the INSPIRE main computer can determine the temperature of the thruster to find the maximum allowable pressure to ensure that a vapor is in the expansion tank. With this upper limit, the computer can then use this relationship to carefully control the expansion tank pressure to get the desired thrust force.

5.3.2 Specific Impulse

The formula for specific impulse is given by the following, where \dot{m} is the mass flow rate of the propellant and g is gravity on Earth’s surface.

$$I_{SP} = \frac{F_{Thrust}}{\dot{m} \cdot g}$$

The thrust was calculated with the ballistic pendulum. The mass flow rate had to be determined in a separate test. Because the flow rate depends on the pressure in the expansion tank, long, multi-second pulses are not the best way to estimate the mass flow rate. Instead, the thruster was massed, placed into the chamber, and fired for 1000 20ms pulses for a total of 20 seconds of open time at room temperature. The pressure was maintained in the expansion tank at a PADC value of 415. The thruster was then removed and massed to

find the total mass change. This was done three times and showed an average mass loss of $1.867 \frac{g}{20s}$ or $0.0933 \frac{g}{s}$. Using the total PADC 415 thrust value of $63.5mN$, this gives a specific impulse of $69.4s$ at room temperature ($20.6C$).

The specific impulse will change with temperature, as the maximum pressure increases in the expansion tank. This increases thrust as well as mass flow rate. Specific impulse tests were not able to be conducted for the higher temperatures to establish this relationship because of the time constraints of massing the thruster, waiting for the temperature to get to a steady state value (one day), conducting the 1000 pulses, and remassing the thruster several times.

5.3.3 Minimum Impulse Bit

The minimum impulse bit is the fastest valve actuation time multiplied by the smallest generated thrust. To calculate this, the fastest valve timing was reliably determined to be $2ms$ and the smallest tested thrust was $43.3mN$ from the room temperature PADC 200 test. As such, the advertised minimum impulse bit is $0.087mN \cdot s$. This can be smaller if the pressure is kept lower in the expansion tank but was not able to be investigated further; the limiting factor is the resolution of the rotary encoder being able to detect even smaller pulses.

5.4 Analysis of Results

The collected thruster data shows strong trends in the performance of thrust generated versus valve time and thrust generated versus expansion

tank pressure. The linearity of the thrust versus PADC value shows that even somewhat noisy data can produce a strong trend to draw conclusions from. Use of the *y - intercept* method allows for the true impulse to be determined from the data; this is the most useful data point for the thruster performance because it will always be exhausting into the vacuum of space. Combining all of these methods, Table 5.4 shows a summary of the data at room temperature. The average power consumption is based on a driving voltage of $7.4V$ for the valves with a 10% duty cycle; a higher duty cycle will increase the average power consumption. The theoretical ΔV is based on the performance of the thruster if all the propellant was used for translational maneuvers rather than attitude control. Beyond room temperature, the thrust can be related to pressure through Equation 5.1. The results are encouraging and show strongly correlated trends that can be used to estimate the performance of the INSPIRE thruster under a range of thermal conditions. However, these trends should be expanded beyond the $18^{\circ}C$ thermal difference range that were able to be tested at the TSL. The vacuum chamber at the TSL cannot be chilled below room temperature and the rotary encoder began to give erroneous measurements once the temperature exceeded $45^{\circ}C$. As a result, though the temperature pressure profile is nearly linear for the temperatures tested, this is not necessarily the case for the range of temperatures the thruster may see. This is not a concern for the mission. The embedded heater can keep the expansion tank propellant heated as required, and it is always easy to maintain a pressure lower than saturation pressure within the expansion tank. This allows the INSPIRE satellite to actively keep the thruster in the known

| Performance Metric | Result |
|--|-------------------|
| Maximum thrust | $63.5mN$ |
| Minimum measurable thrust | $43.3mN$ |
| Specific Impulse | $69.4s$ |
| Fastest valve time | $2ms$ |
| Minimum impulse bit | $0.087mN \cdot s$ |
| Average power consumption (10% duty cycle) | $0.53W$ |
| Total ΔV (theoretical) | $31.4\frac{m}{s}$ |

Table 5.4: Room Temperature Performance of the Thruster

operating region shown by these results.

The post-processing of the results also highlighted the timing and precision errors seen during the testing portion of the data collection. These timing issues are not an issue with the thruster valves or electronic controller and can be directly traced back to the resolution of the rotary encoder as well as the scheduler and accuracy issues with the Linux scheduler on the Phytex SOM. Unfortunately these issues were not able to be resolved before or during the FTT testing and resulted in about 20% of the collected data points being excluded. The following chapter includes a section on suggested improvements for the test stand resolution and computer timing issues. Once these timing issues are resolved, the true minimum impulse but can be calculated by driving the expansion tank pressure low and sampling faster and faster valve timings until the unit no longer produces a measurable force.

Beyond the timing issues, more data points need to be taken to see how the specific impulse is affected by temperature. When taking the mass difference with a scale, a single round of thermal testing for specific impulse would take almost two days per sample, and multiple samples would be re-

quired for each temperature. This is incredibly burdensome. Alternative ways to measure the mass flow rate are also discussed in the next chapter. In the end, the relationship between temperature and specific impulse needs to be characterized to fully understand the performance of the thruster unit.

When comparing the INSPIRE unit to past units, there are similar performance traits between thrusters. Because they used the same propellant, the Bevo-2 and INSPIRE units showed some common results; the Bevo-2 thruster was shown to have a specific impulse of $\sim 60s$ [14]. Unlike the CG ACS units, the Bevo-2 thruster was designed for ΔV maneuvers and generated an average thrust of $\sim 100mN$ with a minimum impulse but of $\sim 1mN \cdot s$. The Bevo-2 showed an exponential relationship between temperature (and thus expansion tank pressure) and thrust, but this was over a $60^\circ C$ range, compared to $18^\circ C$ on INSPIRE. As a follow on to the INSPIRE research, the Bevo-2 thruster is going to be recharacterized with the Flight Test Stand and heater assembly.

Chapter 6

Lessons Learned and Recommendations

Two fully-functional printed cold gas attitude control system thrusters were delivered to JPL. The inclusion of the pressure and temperature sensors, the embedded heater, closed-loop filling system, and dedicated safety and control electronics advanced the state-of-the-art of the thruster systems to the next level. By controlling the temperature and pressure within the expansion tank, the INSPIRE main computer can control the valve actuation times carefully to achieve the desired torques for the mission. With this control and sensing ability, the INSPIRE system is considered a more “intelligent” version of the Bevo-2 system that had no feedback. This chapter discusses future ideas and challenges as the INSPIRE system evolves into an intelligent and independent 6-DOF attitude control module.

6.1 Lessons Learned

The result of the research was successful and several important lessons were learned through the process. Beyond the part selection challenges and computer timing issues already presented, the thruster units showed an amazing durability through testing. The FTT was thermally cycled many times and a single valve registered over 15,000 pulses during the testing period. The

plastic showed no signs of deformation or contamination during the testing period and the o-ring seals were effective in preventing leaks through a simple compression fit. In the final rounds of testing, the FTT spent two straight weeks under a hard vacuum. The assembly of each of the units was quick but proved to be a robust design that showed no noticeable leak. These observations add confidence to the development of the technology. It highlights the fact that a printed thruster designer can rely on their skills and intuition as they design the complex plastic manifolds and implement new sensor suites for different missions.

One of the biggest unanswered questions is related to the fast performance of the Lee Company valves. At best, the fast valve timings from the Phytex SOM were erratic and unpredictable because of the supporting hardware. The TSL did not have a real-time system that could be integrated in time to verify the timing accuracy questions. Overall it was determined that the timing issues did not affect the validity of the measurements. These errors introduced more noise that had to be filtered out, but still showed strong trends relating expansion tank pressure to thrust. Answering these performance questions will be important as a smaller impulse bit and more accurate thrust is requested from printed thruster units on future missions.

Another lesson learned is related to the filling procedures. The vacuum filling method works for the INSPIRE units and allows them to be filled within the P-PODs. However, unlike almost every other component involved with the thruster units, the filling mechanisms and procedures have never been iterated past the baseline design. As higher performance propellants are included in

the printed CG systems, a more robust filling system needs to fill the units quicker with less sophistication. This should be one of the first design trades conducted on future design units; the filling and draining components have proven to be some of the hardest challenges to debug by not being able to see into the Bluestone thrusters.

In the end, one of the biggest, positive lessons learned was related to the scalability of the systems. As new challenges arose related to the selection of different metal-to-metal fittings, the inclusion of the filling port, or the orientation of the nozzles, the printed cold gas technology showcased the ability to rapidly iterate to meet the changed requirements. This is a trait not commonly shown by other satellite subsystems without a significant change in complexity or cost. This is promising for the technology as the TSL continues to iterate and improve on the printed cold gas thruster technologies.

6.2 Designs beyond INSPIRE

The evolution of the printed CG thruster technology from Bevo-2 to INSPIRE shows that the technology processes can be quickly and effectively adapted to different spacecraft. This section looks into how the thruster design can be adapted to other vehicles, as well as the features future iterations may have.

6.2.1 Adapting the Design for Other Missions

The INSPIRE thruster met the requirements initially laid out by the JPL team while showing a flexibility to adapt to design changes. Specifically,

the request to add the nozzle cant angle on all four nozzles highlighted how significant changes were made quickly and easily as the design evolved from the EDU to the FTT. Working with a solid plastic manifold offers this flexibility, and new units can be printed until the final flight integration of the thruster module. The 3D printed CG units also follow a different design rationale than traditional hardware components. Rather than dictating a size to the customer, a printed thruster is able to make-do with the volume afforded to the subsystem by the customer. This makes the technology flexible and extremely portable to other missions even though the satellite configurations may be significantly different.

Customization of the 3D plastic manifolds for a specific mission requires practice with parametric modeling for printed parts but the units can be iterated relatively quickly. The valve manifold assemblies, filling mechanisms, and sensor suites are virtually interchangeable yet customizable for the customer's needs. The plastic can also be scaled beyond the footprint of a single 3U CubeSat. As 6U or 12U spacecraft become more commonplace for scientific and technological payloads, larger plastic manifolds are created using the same design and printing procedures already established. Future thruster versions that require a 4-DOF thruster system may also benefit from having two expansion tanks. Generally a high pressure is desired for ΔV maneuvers because the thrust should be large, while a lower pressure expansion tank would make sense to achieve the smallest rotational torque.

The electronic and power interface with the printed CG units is also very flexible. In the future, the systems can be configured to be independent

as desired by the host spacecraft. The Bevo-2 and INSPIRE main computers control the thruster behavior. Future thruster systems can easily incorporate their own microprocessor to receive, process, and acknowledge high-level commands to execute different maneuvers. These truly embedded systems would manage the propellant's saturated state, pressure, and temperature to achieve the commanded thrust. The data interface between the thruster module and the satellite can be any data bus specified by the host satellite.

6.2.2 Scaling the Technology

The next logical step for the technology is to evolve the CG ACS system into a fully integrated attitude determination and control (ADC) suite. The TSL has baselined a 16-nozzle design that would provide a full 6-DOF for a mission shown in Figure 6.1. By including sensors such as gyroscopes and accelerometers, a dedicated micro controller would have the ability to create and measure its own translational or rotational maneuvers. The main satellite would be responsible for commanding a desired rotation for translation and the CG ADC system would use its own algorithms to correctly direct the propellant out of specific nozzles to achieve the new state.

A full ADC system could be further improved by including more sensors, such as a sun sensor or a star tracker, to create a fully separate attitude control system. Similarly to how the INSPIRE system was configured for a specific spacecraft, a 6-DOF thruster unit would have a basic valve and sensor design that could be integrated with a custom designed plastic manifold. This allows the manifold to fit around other hardware components or support a spe-

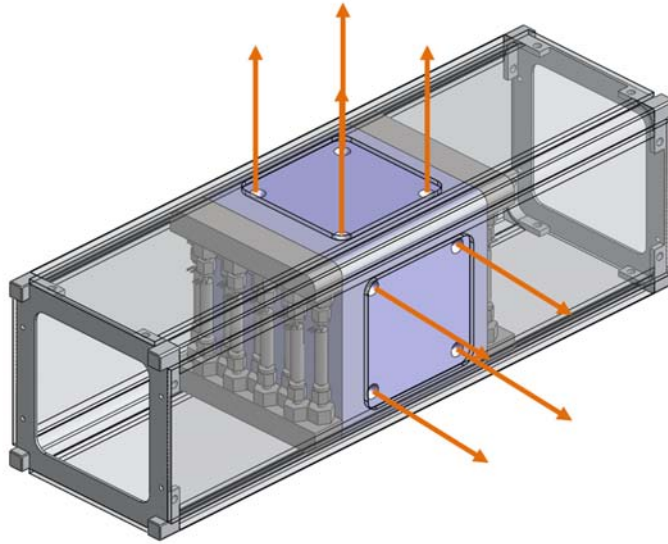


Figure 6.1: A baselined 1U 6-DOF thruster

cific scientific payload. As CubeSats go beyond Earth and mission lifetimes get longer, the volume allocated for these thruster units can grow and directly add to the amount of propellant carried for the mission.

These systems are close to becoming a reality. However, as of May of 2014, neither the Bevo-2 nor INSPIRE thrusters have flown to demonstrate that the technology delivers the laboratory-observed performance. With heritage, fully integrated 3D printed CG ADC modules will compete with or complement traditional and expensive reaction reaction wheel systems as low-cost and low-power actuators for CubeSat missions

6.3 Further Investigations

The design, development, and validation of the INSPIRE ACS units was a requirement driven process that produced two flight units. Because flight deliverables were required from this research, there were other potential improvements to the thruster design that were intentionally ignored to keep the cost, schedule, and hardware delivery risk to a minimum. This section presents some of the possible investigation topics that were not explored.

6.3.1 New Materials and Manufacturing

3D printing is starting to become a household commodity as products like the MakerBot become affordable and readily available to consumers [27]. These systems use the same type of stereolithography technology used to print the Bluestone but currently lack the precision, accuracy, and repeatability seen in high-end commercial products. While the MakerBot targets individual consumers, the whole additive manufacturing through printing field is growing to accommodate industries that might benefit from the benefits of lightweight, strong 3D printed pieces. Accura Bluestone was specifically developed for “high-performance applications”, such as wind-tunnel testing, under-the-hood automotive components, and assembly components [12]. First introduced in 2008, Bluestone has been baselined for UT Austin’s thrusters over many years. Newer materials, such as Accura CeraMAX and Somos NanoTool both offer similar strength, rigidity, and temperature deflection properties of Bluestone but have additional features; the NanoTool material has a very low water absorption percentage and can be printed in layers half as thick as Bluestone

[28]. This allows for finer features to be resolved in the printing process and more complex shapes can be created. Similarly, the CeraMAX material offers the highest strength out of these three plastics and has the lowest density, though it is more expensive than Bluestone [29].

Direct metal laser sintering (DMLS) technologies are also evolving with plastic technologies. In a DMLS system, a powdered metal and alloy material is selectively melted to create solid metal parts. This technology give the parts the strength of a metal but can still generate shapes that could not otherwise be created with a traditional removal machining process. Current production sintering materials include aluminum, stainless steel, titanium, and nickel alloys [30]. This would allow propellant manifold walls to be made thinner to support the same internal pressure. Because these materials are metal, the density is significantly higher than using plastic materials. The sintering also leave the product with a rough finish, which would create flow turbulence within the internal piping and make o-ring seals more challenging.

Another potential improvement in the 3D manufacturing process is the inclusion for “third-party” components during the printing process. For example, on the INSPIRE ACS units, the pressure transducer, temperature sensor, and heater are all secured in a brass plate that is then sealed over the expansion tank. This requires a large o-ring and potentially increase the number of places a leak could occur. Though it is not a commercially available option yet, if electronic materials are embedded into plastics during the printing process then there would be no need for additional passthroughs; in the case of the INSPIRE system, the pressure sensor, heater, and thermistor could all

be printed into a completely enclosed expansion tank and only allow the signal and power wires to pass through. Likewise, the plastic could be printed around the valves, allowing the metal manifolds and metal to metal fittings to be removed to save volume and mass and eliminate leak points.

6.3.2 Improved Test Stand

The limitations with the flight and FTT test stand necessitate the need for a higher fidelity test collection system. Instead of a 10 – *bit* encoder, using the 12 – *bit* pulse-width modulated version of the same encoder will allow measurement of smaller impulses with quadruple the resolution. Additionally, with the degradation of the encoder’s lubrication, a vacuum-rated encoder may also be a consideration.

Some improvements can be made with changes to the design of the test stand. A more balanced pendulum would move the center of mass closer to the fulcrum and encoder. This will allow the pendulum to sweep through a larger angle for a given impulse, so smaller impulses can be measured. While this will reduce the pendulum’s ability to measure large pulses, the pendulum mass can be designed to be “tuneable” depending on the test environment. By configuring it as a heavier pendulum, the pendulum will stay closer to the nozzle exit plane during the pulse, so the impulse approximation will be more accurate. Removing weight would offer the same benefits for smaller pulses.

A third methodology for measuring thruster data would be to integrate an additional pressure sensor onto the vacuum chamber. A pressure sensor with a high sampling rate would allow the specific impulse to be mea-

sured on a pulse-by-pulse basis; the pressure sensor could measure the total pressure change of the known vacuum chamber volume and estimate the mass expelled. The test stand also had to straddle the heating and temperature measuring plate previously designed in the TSL for other research. An integrated temperature sensor and heater platform designed for these units would allow for controlled, uniform heating of the thruster.

Finally, controlling the thruster through LabView instead of a Linux system would synchronize the firing of the thruster with the collection of the data. Currently a user has to initialize the data collection and fire the thruster during the sample period. Using LabView would automate the process and hopefully eliminate the timing issues seen in Chapter 5.

6.3.3 Miniature Components

With the requirement to design and implement a closed-loop filling system for the INSPIRE, a quick trade study was done to determine the best components available on the market. In general, these parts are very hard to find and highlight the need to find more distributors or learn how to make these components in-house. Unlike the miniaturization of electronic components that has benefited the development of small satellite systems, there is no demand for truly miniature pressure components. A search for a miniature metal-to-metal fitting will highlight a part over an inch long, which cannot fit within a satellite less than four inches wide. Small components do exist and have been manufactured for CubeSat applications, but the parts are often custom designed and expensive . For the assembly of the FTT and flight

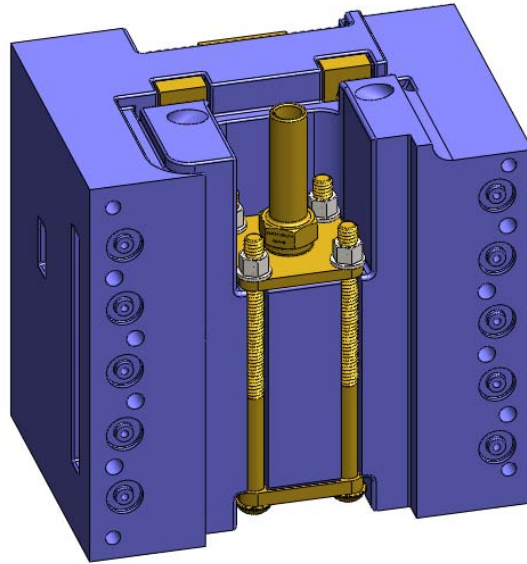


Figure 6.2: The FTT fill valve and volume cutout

units, only one manufacturer was found that specifically made miniature pressure components. Even then, the smallest applicable “fill and drain” valve was used. Figure 6.2 shows how much volume of the INSPIRE thruster was dedicated just to house the fill and drain port.

Miniature, high performance sensors are also not readily available. To embed the thermistor and heater components into the expansion tank, custom machined housings were created and then sent off to a third-party company to pot the cartridge heater and thermistor into the probe housings. This custom work was very expensive. The miniature pressure sensor was a commercially available product, but the application was clearly not geared towards small, volume constrained applications. While the sensor was capable and small, the transducer wire harness included a large and undocumented Wheatstone bridge and tuning circuit board that had to be fit into the thruster plastic

manifold. As more sensors are included in future 3D printed CG thruster systems, size and performance challenge will have to be addressed.

6.3.4 Long Term Duration Tests

The INSPIRE mission concept of operations is unique because the mission will only last a matter of weeks before the satellite are beyond radio contact. Preliminary attitude estimates also indicate that the satellite will only use a fraction of the 180g of propellant stored within each thruster unit. As a result of this, the research with the INSPIRE units did not focus on long term tests that might affect the performance of the system. With the development of the 3D printed CG technology, long term leak and compatibility tests need to be conducted on these thruster systems as missions begin to have longer lifetimes in orbit or venture on longer missions to the moon, near Earth asteroids, or other planets.

The TSL has conducted some long term compatibility tests with the refrigerant and plastic; most recently, the propellant was sealed into a printed manifold for nine months. When the manifold was emptied, the fluid showed no change in color and the interior of the plastic showed no deformation or discoloration. For the INSPIRE units, each flight unit was leak checked by subjecting each assembly to a high vacuum for a day and measuring the total mass difference. The FTT unit was vacuumed for over two weeks and also showed a negligible mass loss ($< 0.1g$). However, everything leaks. While some leak rates may be acceptable for certain missions, this information needs to be quantitatively assessed to determine if the CG thruster design can be

improved upon.

Other long term tests should focus on the behavior of the material in the space environment. For example, for missions outside of low Earth orbit, the affect of different types of radiation on the plastic is currently unknown. Additionally, no formal outgassing tests have been conducted on the plastics. Samples of the different materials mentioned above should be sent to a lab and have the Collected Volatile Condensable Materials (CVCM) and Total Mass Loss (TML) percentages measured and compared to other acceptable substances.

6.4 The Thruster Model

After the delivery of the flight units, a model was created based on the design and performance data from both the Bevo-2 and INSPIRE units. This model currently takes in over a dozen parameters that can be used to tweak the predicted performance characteristics of a thruster. Most importantly, it can take any user supplied volume available in a spacecraft and produce working estimates for a preliminary design. The model calculates useful data such as the dry and wet masses, affects of different propellants, and changes for using different 3D printed materials as well as total achievable ΔV and pulses over the lifetime of a mission. For example, a thruster will only provide ΔV , only two valves are needed for a single nozzle. The model optimizes this scenario by maximizing the fuel load as well as including heaters to raise the total thrust produced. Likewise, the model can lead to estimates for how much propellant would be needed for attitude control for a certain length mission.

The model is in its first version. With the additional processed data from the INSPIRE units, the model will be updated to reflect performance data versus temperature and pressure. The next version will also allow the user to approach the design process from either end; for example, a desired ΔV can be plugged in to generate a thruster size, or a performance for a specified volume can be calculated. In the end, as more thrusters are designed, built, and tested the model will incorporate the data to improve the fidelity of the results.

Chapter 7

Conclusion

CubeSats are revolutionizing the exploration and commercialization of space. Starting as university projects over a decade ago, CubeSats are now being used to conduct meaningful science and technology demonstration missions that were once reserved for flagship missions. The availability of low-cost and mass-produced electronics has led to a rethinking of other hardware systems to find cheaper alternatives that meet the performance requirements of a satellite. The 3D printed cold gas attitude control system is one of the technologies that will be able to supplement or replace traditionally expensive attitude control systems. The printed plastic manifold allows these systems to be custom designed to the spacecraft. Nozzles can be added or subtracted, rearranged, and adjusted to satisfy the ΔV or attitude requirements of CubeSats. With flight heritage, these systems will begin to become more common. With further refined electronic sensor and controls, improvements in printing and thrust characterization, and use of new propellants, 3D printed cold gas thruster modules will play an important role on CubeSats both within Earth orbit and beyond.

Bibliography

- [1] Mehrparvar, A., *CubeSat Design Specification*, Revision 13, The CubeSat Program, Cal Poly SLO, February 2014: http://www.cubesat.org/images/developers/cds_rev13_final.pdf.
- [2] Megale, M., “NanoRacks Successfully Deploys Two Small Satellites from the International Space Station”, NanoRacks, February 11, 2014: <http://www.nanoracks.com>.
- [3] Texas Spacecraft Laboratory Facebook Photostream: <https://www.facebook.com/UTSatLab/photos.stream>, Accessed April 2, 2014.
- [4] NanoRacks Photostream: <https://www.flickr.com/photos/nanoracks/>, Accessed April 5, 2014.
- [5] Platt, J., *NASA Announces New CubeSat Space Mission Candidates*, California Institute of Technology, Jet Propulsion Laboratory, February 2013: <http://www.jpl.nasa.gov/news/news.php?release=2013-073>.
- [6] Hinkley, D., *A Novel Cold Gas Propulsion System for Nanosatellites and Picosatellites*, 22nd AIAA/USU Conference on Small Satellites, August, 2008.
- [7] Kjellberg, H., *Design of a CubeSat Guidance, Navigation, and Control Module*, Masters Thesis, The University of Texas at Austin, August 2011.

- [8] Arastu, S., “Radiometer Atmospheric CubeSat Experiment (RACE)”, Internet, 2014, California Institute of Technology, Jet Propulsion Laboratory: <http://phaeton.jpl.nasa.gov/external/projects/race.cfm>.
- [9] Mueller, J., Hofer, R., & Ziemer, J., *Survey of Propulsion Technologies Applicable to CubeSats*, California Institute of Technology, Jet Propulsion Laboratory, May 3, 2010.
- [10] Image Credit: <http://www.compositesworld.com/articles/the-rise-of-rapid-manufacturing>.
- [11] “SLA Prototypes”, Internet, 2014, Interpro Models: <http://www.interpromodels.com/>.
- [12] “Accura Bluestone Plastic”, Data sheet, 3D Systems Corporation, 2008.
- [13] “Bevo-2 Critical Design Review”, Presentation, Texas Spacecraft Laboratory, November 14, 2011.
- [14] Arestie, S., Hudson, B., & Lightsey, E. G., *Development of a Modular, Cold Gas Propulsion System for Small Satellite Applications*, The Journal of Small Satellites, Volume 1, No. 2, October 2012.
- [15] Klesh, A., “Interplanetary NanoSpacecraft Pathfinder In a Relevant Environment”, Presentation, CubeSat Developers Workshop, April 2013.
- [16] Klesh, A., et. al., *INSPIRE: Interplanetary NanoSpacecraft Pathfinder In Relevant Environment*, 27th AIAA/USU Conference on Small Satellites, August, 2013.

- [17] "FE-36 Product Brochure", Data sheet, DuPont, 2005.
- [18] "Thermodynamic Properties of HFC-236fa", Data sheet, DuPont, 2005.
- [19] "Fracture Control Requirements for the Payloads Using the Space Shuttle", Technical Standard NASA-STD-5003, NASA, October 7, 1996.
- [20] "Thermodynamic Properties of HCFC-123", Data sheet, DuPont, 2014.
- [21] "Thermodynamic Properties of HCFC-124", Data sheet, DuPont, 2014.
- [22] "Thermodynamic Properties of HFC-134a", Data sheet, DuPont, 2014.
- [23] "Extended Performance Solenoid Valve", Data sheet, The Lee Company, May 2010.
- [24] "Subminiature Flush Diaphragm Pressure Transducer", Data sheet, Omega Engineering, 2014.
- [25] "Screw Type Quick Disconnect", Data sheet, Beswick, 2014.
- [26] Meirovitch, L., "Fundamentals of Vibrations", Waveland Press Inc., 2010.
- [27] "Replicator 2 Desktop 3D Printer", Data sheet, MakerBot.
- [28] "Product Data Sheet Somos NanoTool", DSM Functional Materials, 2012.
- [29] "Accura CeraMAX Composite", Data sheet, 3D Systems Corporation, 2010.
- [30] "Additive Materials (DMLS)", Internet, 2014, Harvest Technologies: <http://www.harvest-tech.com/additive-metals.php>.

Vita

Travis Kimble Imken attended The University of Texas at Austin and received his Bachelors Degree in Aerospace Engineering with Highest and Special Honors. Upon completion of his Master's degree, Travis will start as a Systems Engineer at the NASA Jet Propulsion Laboratory in Pasadena, California.

Permanent contact: imken@utexas.edu

This thesis was typeset with \LaTeX^\dagger by the author.

[†] \LaTeX is a document preparation system developed by Leslie Lamport as a special version of Donald Knuth's \TeX Program.